University of Stavanger

Faculty of Science and Technology

MASTER'S THESIS

Study program/ Specialization: Petroleum Engineering/ Production Engineering	Spring semester, 2011 Open
Writer: **Adri Maijoni**	…… (Writer's signature)
Faculty supervisor: **Prof. Aly Anis Hamouda** External supervisor(s):	
Titel of thesis: **Mechanistic Study of CO_2 Flooding of Aspaltenic Oil Reservoir**	
Credits: 30 ECTS	
Key words: Asphaltene, precipitation, deposition, CO_2 flooding, miscible flooding	Pages: 56 + enclosure: 28 Stavanger, 15th June, 2011

ABSTRACT

Carbon dioxide (CO_2) injection is one of the most common enhanced oil recovery (EOR) techniques to increase the oil production. CO_2 is injected into the reservoir to displace the residual oil left and mobilize the oil to production wellbore. However, CO_2 injection may trigger asphaltene precipitation. Three major factors affecting asphaltene precipitation are pressure, temperature and composition.

Influences of pressure drop on asphaltene precipitation, to our knowledge, has less attention as additional factor that play roles in precipitated asphaltene.

The main objective of this study is to investigate the effect of pressure drop on asphaltene precipitation. The investigation is done at laboratory for different flowing pressure and temperature. It is shown that higher pressure drop gives higher amount of asphaltene precipitation. When comparing to the effect of flowing pressure, it is interesting to see the pressure drop affects asphaltene precipitation but not the flowing pressure.

TABLE OF CONTENTS

LIST OF FIGURES

LIST OF TABLES

ACKNOWLEDGEMENTS

First and foremost, I thank God, Allah SWT, for answering all my prayers, and giving me the strength to complete this study.

I would like to express my deepest thanks to my supervisor, Prof. Aly Anis Hamouda for his unfailing encouragement, support and advice throughout this study. His sincere dedication, generosity and willingness to exchange ideas where crucial in the development of this study were remarkable. I would also like to express my deep gratitude to Vahid Tabrizy, for giving me a chance to learn more about running an experiment through his wise counsel and assistance.

I am thankful to all of my professors and lecturers, during my course work in the Master program, for their contribution in my thinking and understanding on various issues on petroleum engineering. My thanks also go to my fellow Master students, for their willingness to work together and support one another.

With love and deep appreciation, I acknowledge my wife, Meghi Tressa for the prayers, support and encouragement. Without her love, affection, and sacrifices, this study would not have been accomplished. I am grateful to my late father Abdul Ghafar and my mother, Ibunda Nettiwarti for instilling me the love of learning and the belief that almost anything can be accomplished through hard work and determination.

Finally, I would like to thank all of my Indonesian friends in Norway and all of my relatives in Indonesia (Talu, Bukittinggi, Padang, and Jakarta) for their endless support.

Stavanger, 15th June 2011

Adri Maijoni

1 INTRODUCTION

1.1 Background

Petroleum has fueled the world's energy needs for the past century. Today, rapid industrialization in once-developing countries, such as China and India, is dramatically increasing worldwide oil consumption. In 2010 Global oil demand reached an average of 87.9 mb/d (+3.4% or +2.9 mb/d year-on-year) and is still seen rising to 89.2 mb/d in 2011 (+1.6% or +1.4 mb/d year-on-year) (International Energy Agency – Oil Market Report, 12 April 2011). The increasing demand for oil is challenge the oil industry to produce more oil at an efficient cost.

Most oil is produced in three distinct phases: primary, secondary, and tertiary, or enhanced oil recovery (EOR). In primary recovery oil is produced by the original reservoir drive energy but only about 10 percent of a reservoir's original oil in place is typically produced. Secondary recovery techniques extend a field's productive life generally by injecting water or gas to displace oil and drive it to a production wellbore, resulting in the recovery of 20 to 40 percent of the original oil in place. Enhanced oil recovery (EOR) is that something is added to the reservoir after secondary recovery in order to increase the oil production. This can be gases, chemicals, microbes, heat, or even the addition of energy, such as the stimulation of the oil through vibration energy. EOR offers prospects for ultimately producing 30 to 60 percent, or more, of the original oil in place.

Nowadays, the most common EOR techniques in the market is carbon dioxide (CO_2) injection. CO_2 is injected into the reservoir through injection well to displace the residual oil left after secondary recovery

and drive the oil to a production wellbores. CO_2 injection can significantly increase the oil recovery. However, it causes asphaltene precipitation and deposition at high concentrations (Okwen, 2006). Asphaltene is best known for the problems they cause as solid deposit. It can deposit anywhere in the wellbore and production system.

As can be seen in Figure 1.1, asphaltene precipitation and deposition causes plugging of the pore throats near the wellbore, reducing rock permeability and the anticipated rate of oil production. In many cases, the asphaltenes precipitation and deposition can plug up the production tubing or can be carried to the wellhead, through the flowlines and into the separator and other downstream equipment (Yin et al., 2000).

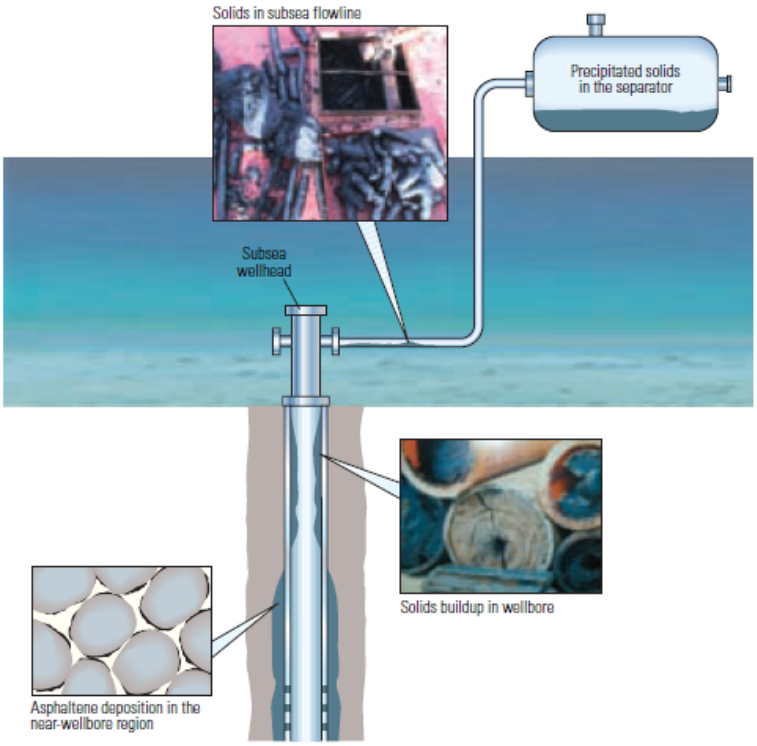

Figure 1.1 Asphaltene precipitation and deposition (Schumberger Oil Field Review Summer, 2007)

The place where the asphaltene problem is most critical is perhaps near the well bores and production tubing. Asphaltene deposition inside the well can restrict the wells and result in production losses. It is also can cause damage to downhole equipment, such as electric submersible pump (ESP) and downhole safety valves (Yin et al., 2000).

The following are two field cases that cause production loss and cost ineffectiveness due to asphaltene precipitation and deposition:

1. Asphaltene Problems in Kuwait (Oskui and Jumaa, 2009)

In late 2009, Kuwait Oil Company (KOC) was facing aphaltene deposition problems in the wellbore. The asphaltene gradually deposits inside the tubing, reducing its diameter and causes production rates to drop and eventually the well completely ceases to flow. Once this has occurred, the tubing in the well must be cleaned out to restore the well to production. The cleaning process takes around 1 month and during this period the wells are completely shut off (production loss of around 50.000 bbl/day).

2. Asphaltene Problems in Venezuela (Schlumberger Oil Field Review Summer, 2007)

In a field in the northern Monagas province of eastern Venezuela, a combination of crude-oil composition and production conditions led to severe pipeline clogging by asphaltenes. Flow testing determined that two pipeline sections totaling 9,300 m in length were completely plugged. Various cleaning options were considered, including high-pressure water blasting, steam and xylene injection, and pipeline pigging units. All were eliminated for technical, environmental and

economic reasons. The other alternative, replacing the pipeline, would cost US $1.4 million and take eight months.

Considering possible loss and cost ineffectiveness resulted from asphaltene precipitation, it is very important to understand the parameter that causes asphaltene precipitation and must be evaluated at early stage of EOR method. Laboratory analysis and field intervention help the operator avoid or remediate asphaltene precipitation and deposition (Schlumberger Oil Field Review Summer, 2007).

1.2 Objective

Although factors affecting the asphaltene precipitation (pressure, temperature, and composition) have been investigated in literature, low attention has been paid to the effect of constant pressure drop. The main objective of this study is to investigate the effect of pressure drop across the core on asphaltene precipitation since it is believed that this factor has more effect than pressure on precipitated asphaltene.

2 LITERATURE STUDY

2.1 Asphaltene

The word asphaltene was introduced in France by J.B. Boussingault in 1837 (Mansoori, 2005). Boussingault described the constituents of some bitumens (asphalts) found at that time in Eastern France and in Peru. He named the alcohol insoluble, essence of turpentine soluble solid obtained from the distillation residue "asphaltene", since it resembled the original asphalt.

Nowadays, asphaltene is known as the heavy fraction of petroleum mixture, which is insoluble in some species such as paraffins but soluble in other such as aromatics (benzene, toluene, etc) (Yin et al., 2000, Zekri et al., 2009, Negahban et al., 2004, Takhar et al., 1995 and Vafaie- Sefti et al., 2002). It is recognized as a black or dark brown colored molecular substance. Asphaltene is heterocyclic unsaturated macromolecules that consist of carbon, hydrogen as primary component and a minor proportion of heteroelements such as oxygen, nitrogen, etc (Yin et al., 2000). The amounts of carbon and hydrogen in asphaltenes vary over a very small range so that the hydrogen to carbon (H/C) ratio is fairly constant at about 1.1-1.2, which is characteristic of a strong aromatic composition (Yin et al., 2000). Over the past decades the molecular weight, molecular structure and the density of asphaltene has been a subject of controversy (Chukwudeme, 2009).

The reported molecular weight of asphaltene varies depending upon the method and conditions of measurement (Mansoori, 2005). A major concern in reporting molecular weights is the aggregation of asphaltenes which can exist at the conditions of the method of

measurement. Figure 2.1 shows one of proposed molecular structure of asphaltene for maya crude in Mexico (Mansoori, 2005).

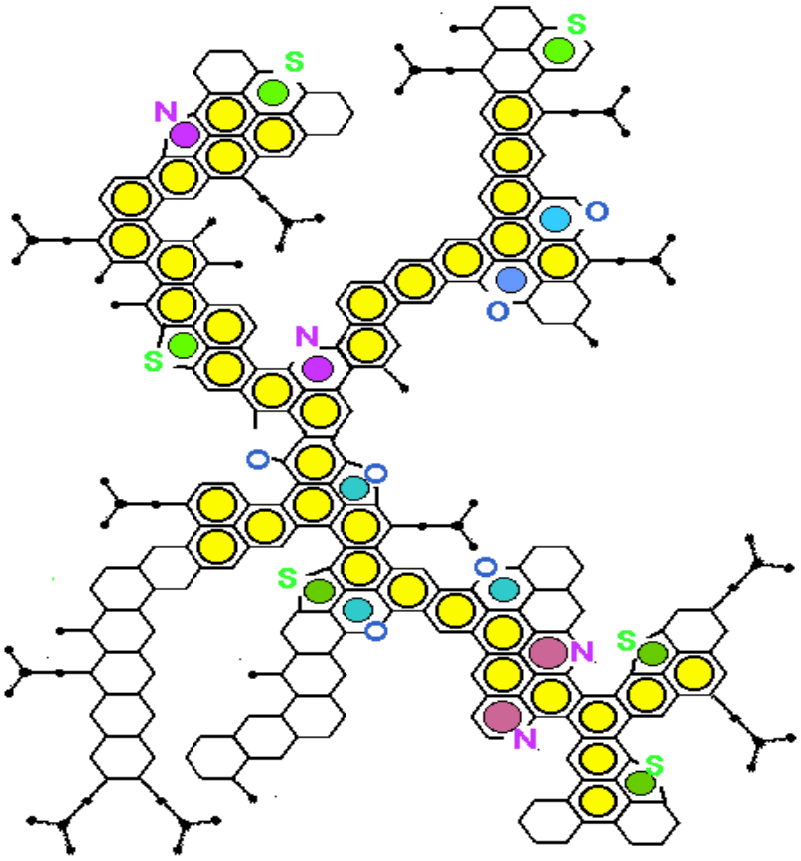

Figure 2.1 Molecular structure of asphaltene proposed for maya crude (Mexico) (Mansoori, 2005)

Asphaltene is generally found in all crude oils. Crude oils which have a low aromatic content have a higher degree of asphaltene instability (Takhar et al., 1995).

Asphaltenes tend to remain in solution or in colloidal suspension under reservoir pressure and temperature condition. They may start to precipitate once the colloidal suspension is destabilized, which is caused by changes in pressure and/or temperature during primary depletion (deBoer et al., 1992). Vafaie-Sefti et al., (2002) also

reported that change in some of the environmental parameters, such as pressure and composition, can change stable condition in oil mixture to some other condition in which the oil mixture will be unstable and finally heavy organics, such as asphaltenes precipitate and deposit.

2.2 Detection method for asphaltene precipitation

The methods or laboratory techniques that have been developed for studying asphaltene precipitation from live crude oil are (Schlumberger Oil Field Review Summer, 2007 and Chukwudeme, 2009):

1. Gravimetric

In this method, precipitated asphaltene occurs when pressure falls below asphaltene onset pressure. Asphaltenes precipitate and fall to bottom of pressure volume temperature (PVT) cell. This method provides data for asphaltene concentration versus pressure plot. Figure 2.2 shows an example of gravimetric detection of asphaltene precipitation in Middle East oil. Asphaltene insoluble in n-pentane and n-heptane are precipitated by SARA (saturated, aromatic, resin and asphaltene) fractionation at the reservoir temperature of 116^{o}C. Both type of asphaltenes showed the same precipitation tendencies.

The accuracy of this method is depending on the selection of pressure steps and accuracy of asphaltene-concentration measurements. Small intervals between pressure measurements give better accuracy. So this method requires large volumes of reservoir fluid and may be time consuming.

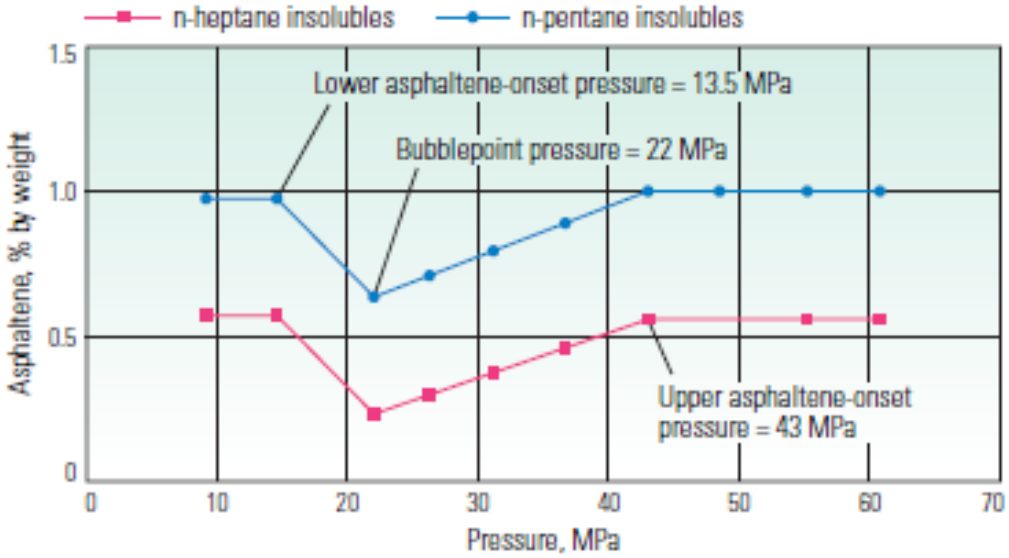

Figure 2.2 Gravimetric detection of asphaltene precipitation in Middle East oil (Schlumberger Oil Field Review Summer, 2007)

2. Filtration

In this method, small amount of fluid extracted from depressurized PVT cell filtered through a 0.22-0.45 μm filter (Milipore). The amount of precipitated asphaltene and the extracted asphaltene could be used for further analysis such as saturated, aromatic, resin and asphaltene (SARA). This method is used in this study.

3. Acoustic resonance technique (ART)

In this method, the changes in the acoustic properties of the fluid as asphaltene drop out of solution are measured. This method is less time consuming and requires low volume of single phase reservoir fluid compared to gravimetric method. However, the resonance changes detected by the ART are not unique to asphaltene precipitation because presence of other solids and vapor-liquid phase boundary could cause similar changes in acoustic properties. This method does not allow the fluid to be mixed causes the inaccurate

onset measurements. Also, this method does not detect the lower boundary of asphaltene-precipitation envelope.

Figure 2.3 shows an example of the ART detection of asphaltene precipitation in the same Middle East oil at the reservoir temperature of 116°C. The asphaltene onset pressure obtained by the ART agrees with the results obtained by the gravimetric method.

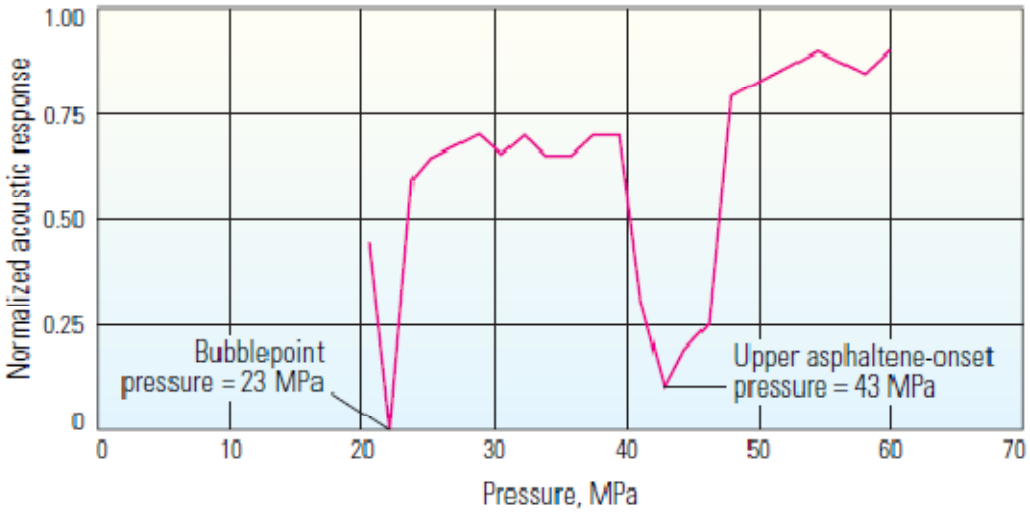

Figure 2.3 ART detection of asphaltene precipitation in Middle East oil (Schlumberger Oil Field Review Summer, 2007)

4. Light scattering technique (LST)

This method uses near infrared light to probe fluids as asphaltene precipitate either isothermally with decreasing pressure or isobarically with decreasing temperature. When asphaltene precipitate, they scatter light, reducing the transmittance power of the light detected by the fiber optic sensors on the other side of the cell. This method is also known as the solid detection system (SDS). As the ART method, this method also requires low volume of single phase reservoir fluid.

Figure 2.4 shows an example of the results of the LST method applied to isothermal depressurization of oil from the Gulf of Mexico. When the pressure decreases from more than 90 MPa, the light transmission power (blue line) increases, because the less dense fluid allows more transmission of light. At a pressure of 37 MPa, light transmittance shows onset of asphaltene precipitation and the upper boundary of the asphaltene precipitation phase envelope (APE). When pressure falls to 33 MPa, light transmittance falls even farther, and at pressure 29 MPa, light transmittance increases as the gas release at the bubble point. With continued depressurization, light transmittance jumps at 26 MPa, when asphaltenes start to redissolve at lower boundary of the APE.

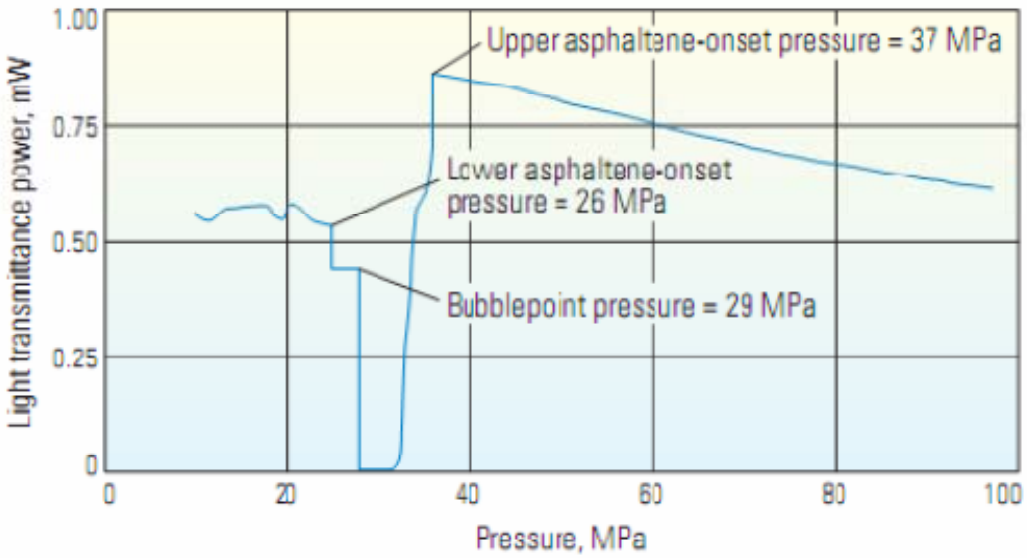

Figure 2.4 Asphaltene-precipitation measurements on oil from the Gulf of Mexico, using the light-scattering technique (Schlumberger Oil Field Review Summer, 2007)

2.3 Factors affecting aspheltene precipitation

Wang and Civan (2005) described that reservoir pressure,

temperature and oil composition are the main factors affecting the asphaltene precipitation in reservoirs during primary oil recovery. However, in this study, the effect of constant pressure drop across the core on asphaltene precipitation is introduced.

Temperature effects are important since the higher the temperature the greater the solubility of the resins in the n-alkenes and therefore the less soluble the asphaltenes in the crude (Zekri et al., 2009). Many studies were conducted on modeling of asphaltene solubility and precipitation. Hirschberg et al., (1984) described that temperature dependence cannot be guessed in general. Thermal expansion of the crude and reduction of asphaltene interaction oppose the 'normal' effect of temperature (increase of solubility upon increase of temperature).

The pressure effect is the major factor on asphaltene precipitation. Moqadam et al., (2009) addressed the experimental results for asphaltene precipitation due to change in pressure and CO_2 composition. As shown in Figure 2.5, above the bubble point, by decreasing the pressure the amount of asphaltene precipitation increases. When the pressure decreases below the bubble point, the amount of asphaltene precipitation also decreases. Figure 2.5 also shows that the maximum amount of asphaltene precipitation occurs at a point close to bubble point pressure.

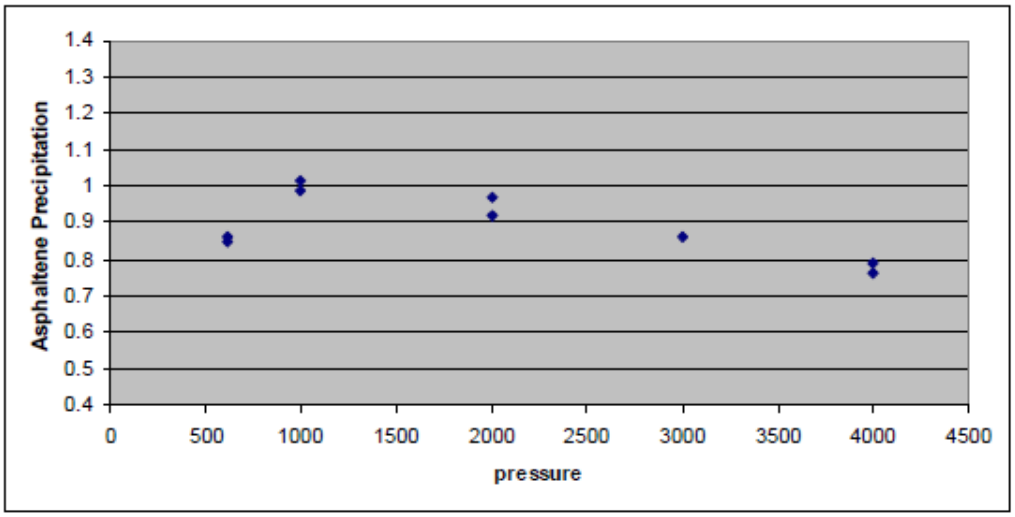

Figure 2.5 Effect of pressure depletion on asphaltene precipitation (Moqadam et al., 2009)

The effect of pressure changes on asphaltene precipitation also can be explained by pressure-temperature (P-T) diagram (asphaltene-precipitation envelope) (Schlumberger Oil Field Review Summer, 2007), as shown in Figure 2.6. For a given initial reservoir condition, primary depletion causes pressure to decrease. When the pressure reaches the upper asphaltene envelope (asphaltene-precipitation onset pressure), dissolved asphaltene start to precipitate. As pressure continuous to decrease, the amount of asphaltene precipitation increases, until the pressure reaches bubble point line and gas come out of solution. With continued pressure to decrease, more gas release from the system causing the oil become denser. These conditions lead to re-dissolution of the previously precipitated asphaltene at lower asphaltene envelope.

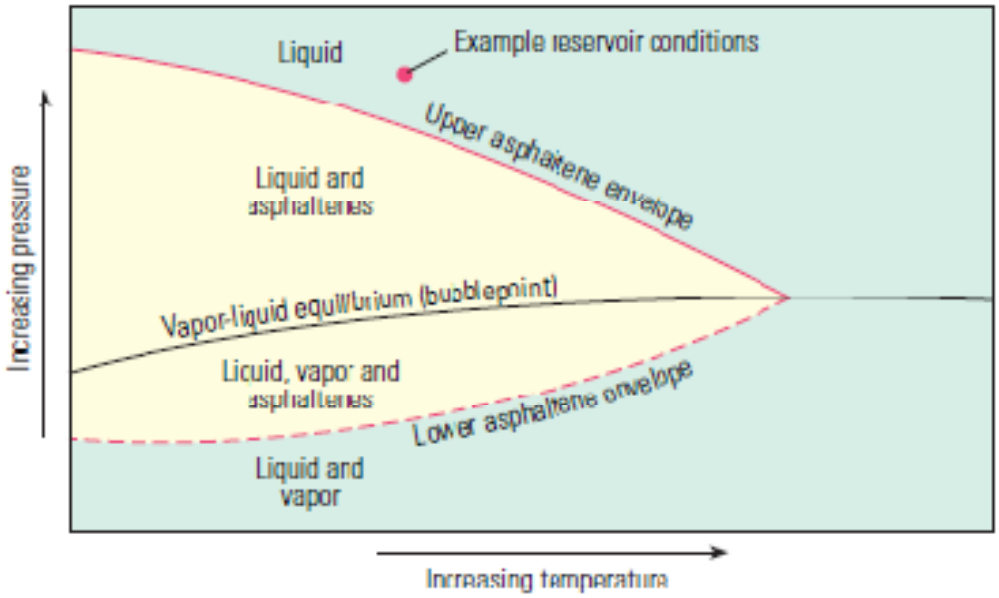

Figure 2.6 Asphaltene-precipitation envelope (Schlumberger Oil Field Review Summer, 2007)

Another factor affecting asphaltene precipitation is the amount of CO_2 injection. As shown in Figure 2.7, increase in CO_2 injection causes increase in the amount of asphaltene precipitation.

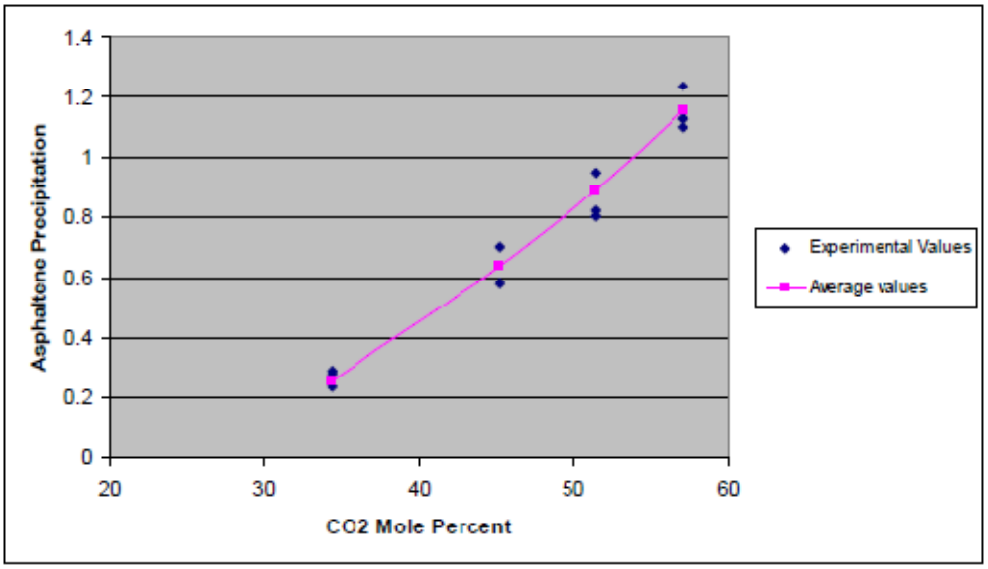

Figure 2.7 Effect of CO_2 injection on asphaltene precipitation (Moqadam et al., 2009)

2.4 Effect of asphaltene precipitation in oil recovery

To increase the recovery from crude oil reservoirs, carbon dioxide (CO_2) is usually injected during secondary and/or tertiary recovery. However, CO_2 injection causes asphaltene deposition at high concentrations (Okwen, 2006 and Zekri et al., 2009). When the critical content of CO_2 is exceeded, the asphaltene deposition occurs. The critical content of CO_2 is a function of oil composition, temperature and pressure (Hamouda et al., 2010).

Asphaltene precipitation causes plugging of pore throats in the reservoir, reducing core permeability and the anticipated rate of production (Okwen, 2006 and Kokal and Sayegh, 1995). Asphaltene precipitation also leads to rock wettability reversal in reservoir rocks. Thus, the adverse effects of both calcite and asphaltene precipitation jointly lead to permeability reduction and subsequently reduction in anticipated rate of production (Okwen, 2006).

In many cases, the precipitation of asphaltenes can plug up the production tubing or can be carried to the well head, through the flowlines and into the separator and other downstream equipment causing expensive problems (Kokal and Sayegh, 1995). Asphaltene deposition inside the well can constrict the wells and result in production losses.

2.5 Refractive index

Refractive index is ratio of the speed of light in a vacuum to the speed of light in a given material. In this study, refractive index is measured by Abbe Refractometer (Carl Zeiss model) to confirm the precipitation of asphaltene in the core. This is done by measuring refractive index

of the sample oil before and after CO_2 flooding. The refractive index will decrease when the sample oil become lighter. Buckley et al., (1998) described that as API gravity increases, refractive index of crude oil decreases, as shown in Figure 2.8.

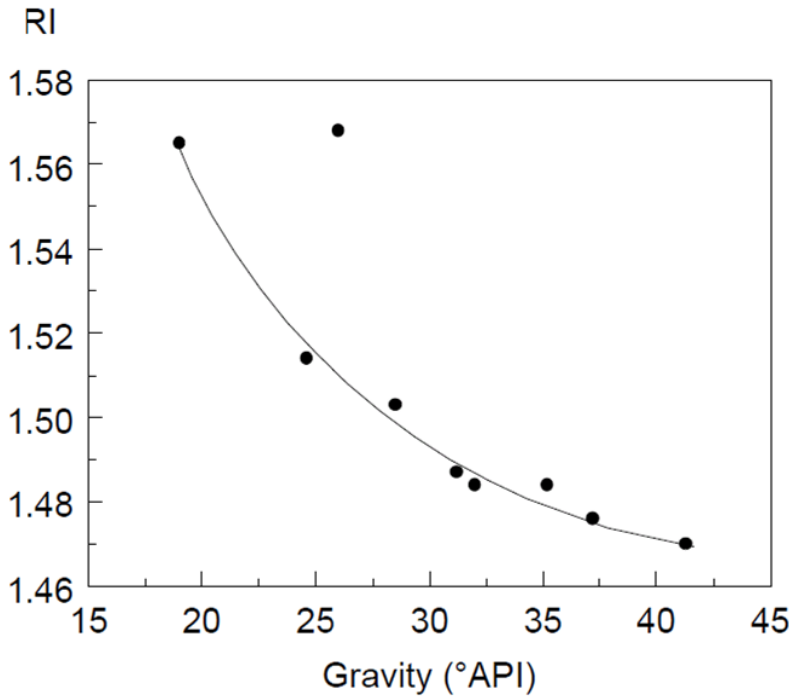

Figure 2.8 Refractive index as function of oil gravity (Buckley et al., 1998)

2.6 Methods to control asphaltene precipitation

Flocculation and deposition of asphaltenes can be controlled using various production and chemical treatment techniques. Production techniques include (Mansoori, 2010):

a. Reduction of shear: asphaltene can flocculate and form under high shear flow conditions.

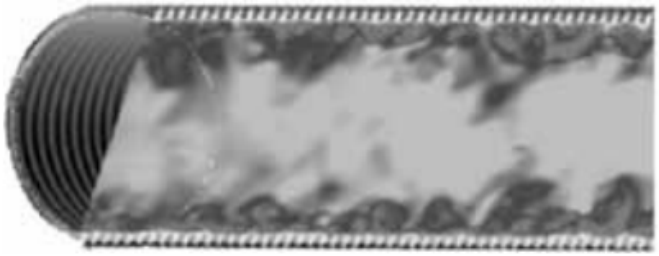

Figure 2.9 Pipe flow with shear

b. Elimination of incompatible materials from asphaltic crude oil streams.

Figure 2.10 Incompatible miscible fluids flow

c. Minimization of pressure-drops in the production facility, causing separation of phases from a miscible phase to oil, gas and heavy organic phase.
d. Minimization of mixing of lean feed stock liquids into asphaltic crude streams

Chemical treatment techniques include: addition of dispersants, antifoulants, and aromatic solvents which may be used to control asphaltene deposition (Mansoori, 2010). Dispersants work by surrounding the asphaltene molecules similar to the natural resin materials. Aromatic solvents for asphaltene deposits need to have a high aromaticity to be effective, and antifoulants have proven effective in condensate stabilization units in gas plants.

2.7 Carbon dioxide (CO_2) injection

Carbon dioxide (CO_2) injection is one of the enhance oil recovery (EOR) methods that is used to increase the productivity of crude oil reservoir. It is usually injected during secondary and/or tertiary recovery.

CO_2 injection is regarded as one of the most efficient oil development methods because CO_2 can enhance oil recovery significantly by swelling oil, decreasing viscosity of crude oil, and reducing interfacial tension between the displacing phase and displaced phase (Lei et al., 2010). It appeared in 1930's and had a great development in 1970's (Yongmao et al., 2004). CO_2 injection from industrial plants emission also provides another beneficial opportunity due to the added value of dealing with global warming and reducing Green House Gas (GHG) emission by CO_2 sequestration and as storage oil / gas reservoirs (Oskui and Jumaa, 2009).

However, CO_2 injection for enhancing oil recovery may trigger asphaltene precipitation because of the interaction between injected gas and heavy components in oil. During gas injection, precipitated asphaltene is composed of strongly polar and strong non-ideal molecules, which results in a liquid-like solid precipitation with strong viscosity under reservoir conditions (Lei et al., 2010). Once the asphaltene precipitation occurs, it causes severe permeability and porosity reduction and wettability alteration, changing relative permeability in the reservoir and, in the severe cases, plugging the wellbore and surface facilities (Oskui and Jumaa, 2009). Figure 2.11 below shows an illustration of CO_2 injection in enhanced oil recovery (EOR) process.

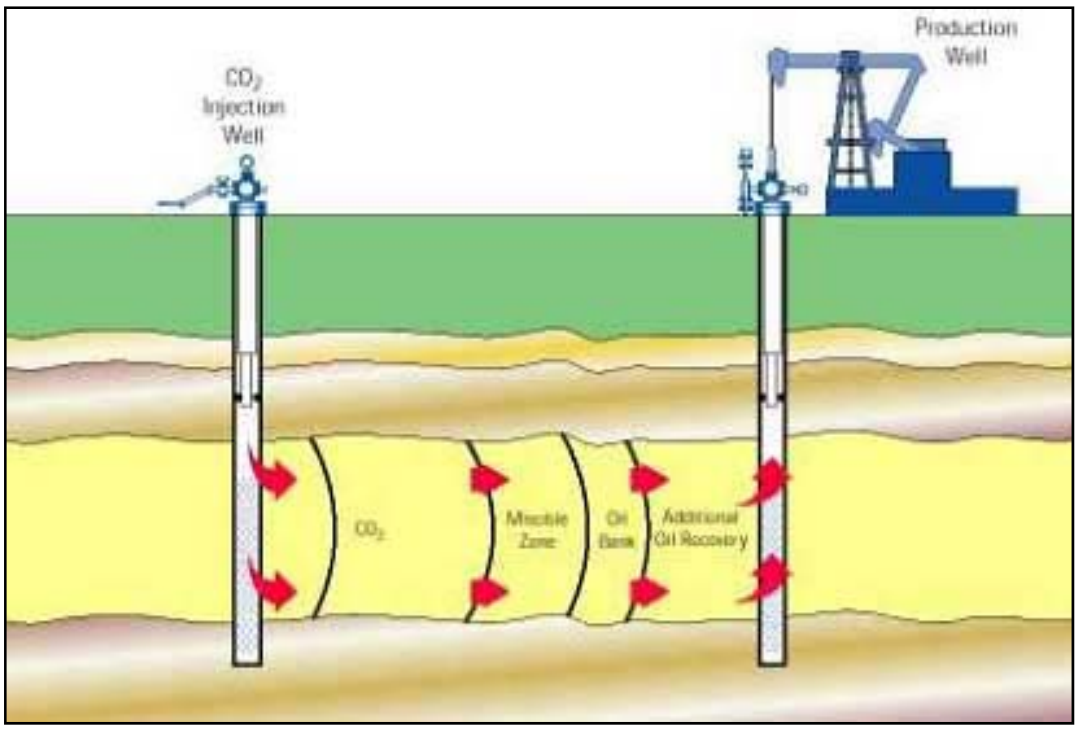

Figure 2.11 Illustration of CO_2 injection enhanced oil recovery (EOR) (Enhanced Oil Recovey Backgrounder)

2.7.1 Miscible / immiscible flooding

In CO_2 injection, miscible flooding processes are defined as processes where the effectiveness of the displacement results primarily from miscibility between the oil in place and CO_2 as displacing fluid. Immiscible flooding processes take place when the injected CO_2 remains distinct from the oil within the reservoir, creating two-phase flow with very high interfacial tension at the surface between these two fluids (Rathmell et al., 1971).

Miscible and immiscible flooding process of crude oil reservoirs by CO_2 is often used in enhanced oil recovery (Yin et al., 2000). When an oil field becomes a candidate for CO_2 flooding, a miscible or near-miscible process is considered to be the most desirable result (Yongmao et al.,

2004). Miscible and or immiscible displacement in CO_2 flooding is controlled by the pressure, temperature, composition of crude oil and composition of the CO_2 as displacing fluid.

During CO_2 flooding of a miscible fluid, CO_2 is injected into the reservoir to displace the residual oil left after water flooding and mobilize the oil toward producing wellbores. In petroleum system, miscible displacement processes is classified into two classes (Rathmell et al., 1971):

1. Processes in which the injected fluid and in-place fluid form a single phase solution for all compositions. This process is characterized as having first contact miscibility, for example propane slug process.

2. Processes in which the injected fluid and in-place fluid do not on a single equilibrium contact form a single phase solution over most of the range of possible compositions, but which may generate a zone of contiguous single phase compositions by multiple contact mass transfer of components between the injected and in-place fluids. These processes are known as multiple contact miscibility, including the enriched gas drive process and the high pressure gas process.

Ternary diagrams are used to describe conceptually the manner in which miscibility is achieved in the multiple contact miscibility processes.

Green and Willhite (1998) described the concept of miscibility based on ternary diagram as shown in Figure 2.12. It shows the phase behavior for the ternary system of methane (C_1), normal-butane (n-

C_4), and decane (C_{10}) at pressure of 2500 psia and temperature of 160°F. At these conditions, all C_1/n-C_4 mixtures are miscible, as are all n-C_4/C_{10} mixtures. Mixtures of C_1 and C_{10} are not miscible over the total concentration range and neither are mixtures of all three components. Any mixture of components that yields an overall composition within the two-phase region is immiscible mixture.

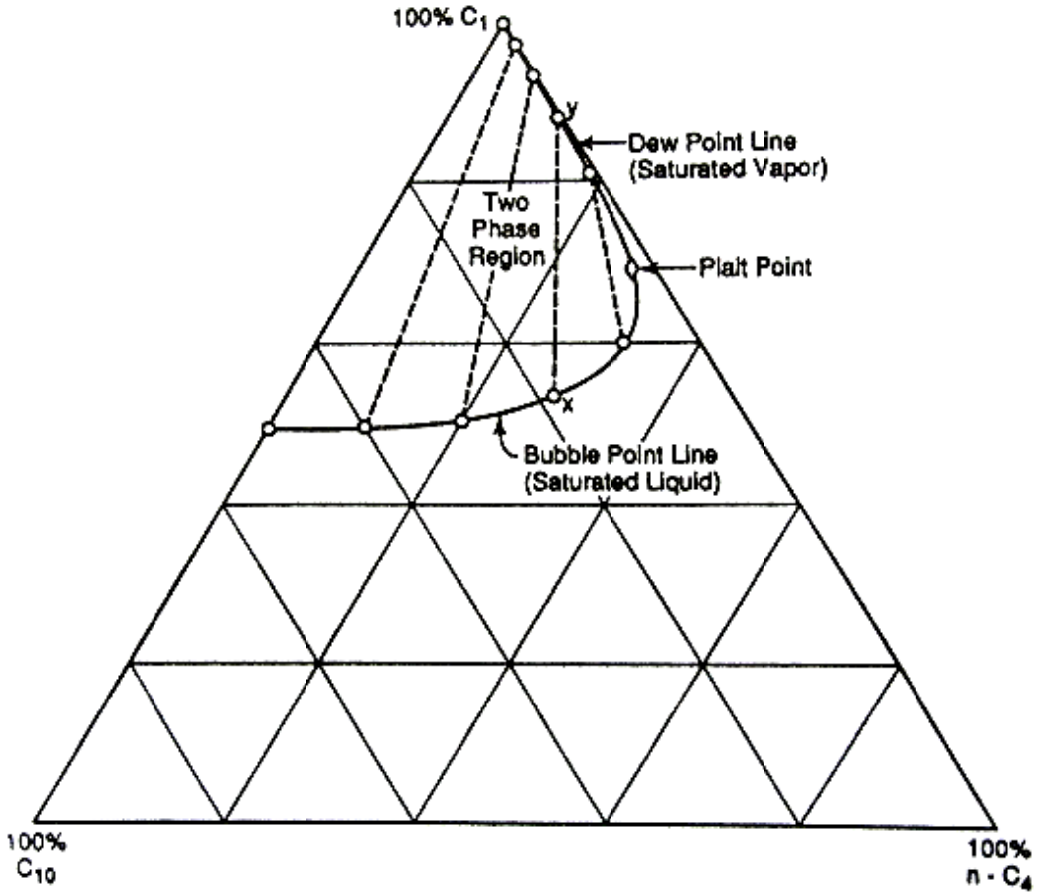

Figure 2.12 Phase relation (mol %) for C_1, n-C_4, and C_{10} system at 160°F and 2500 psia (Green and Willhite, 1998)

2.7.2 Minimum miscibility pressure

In CO_2 flooding, the determination of the conditions at which dynamic miscibility will be achieved for specified reservoir fluids and reservoir

characteristics is an important design consideration. CO_2 flooding above the minimum miscibility pressure (MMP) is a widely practiced means for improving oil recovery in many reservoirs. So it is very important to measure CO_2 MMP at certain temperature. CO_2 MMP is the minimum pressure at which the reservoir fluid is expected to develop multi contact miscibility with CO_2. Generally, reservoir oil composition and temperature are accepted the key factors which greatly influence the CO_2 MMP.

Two laboratory methods used to measure gas-oil miscibility under reservoir condition are the slim-tube method and the rising-bubble method. A large portion of MMPs reported in the literature in recent years were measured with slim-tube apparatus and just a few MMPs were measured with rising-bubble apparatus (Elsharkawy et al., 1996).

A schematic flow diagram of typical slim-tube test equipment is presented in Figure 2.13. MMP is measured by conducting displacement test at different pressure while the other parameters (temperature, injection rate, etc) are kept constant. Recoveries are plotted as a function of displacement test, as presented in Figure 2.14. The MMP is assumed to be the pressure at the 'break' in the curve, i.e. the pressure above which very little additional recovery occurs.

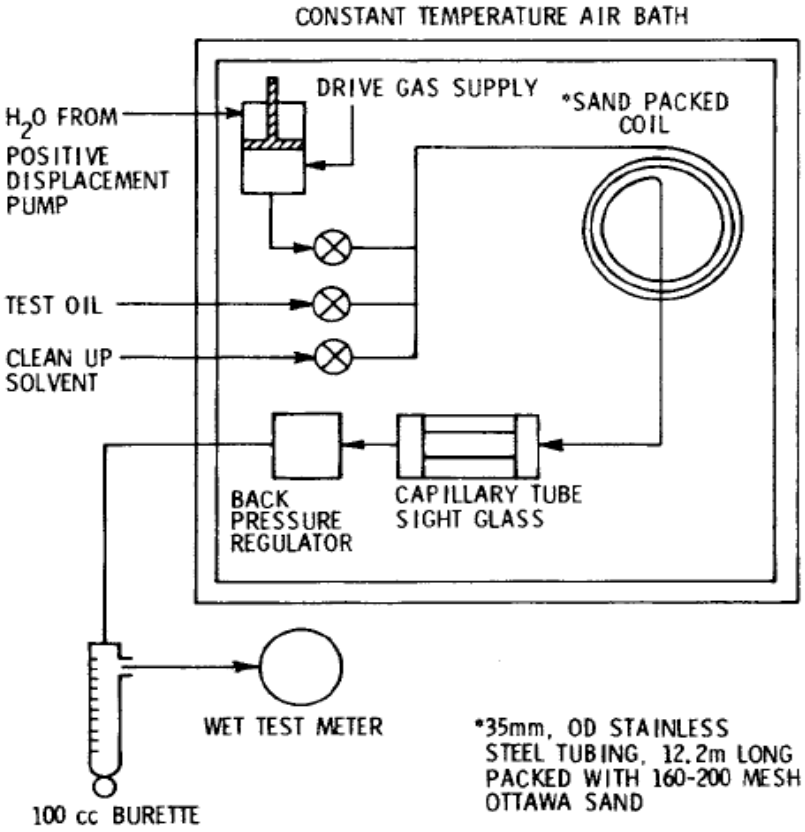

Figure 2.13 A schematic flow diagram of typical slim-tube test equipment (Metcalfe, 1982)

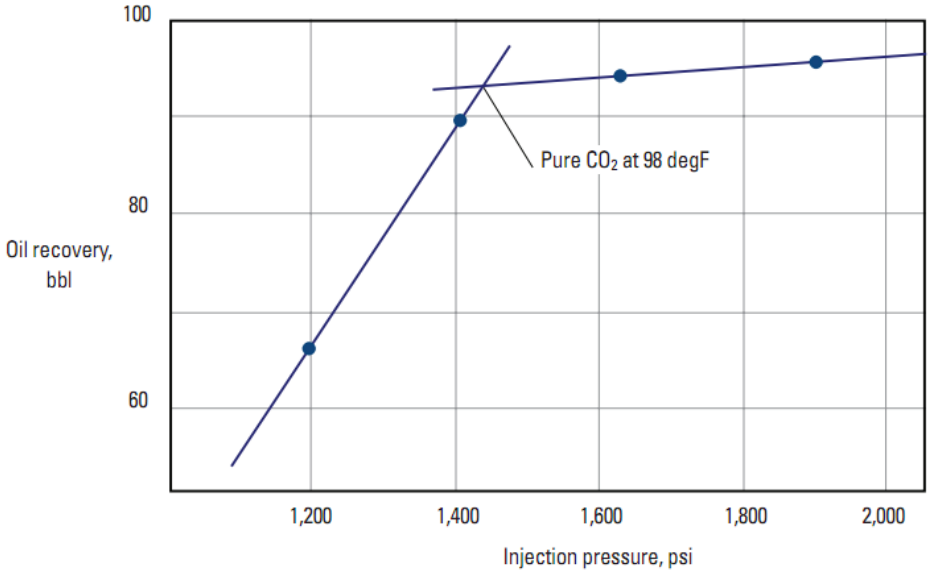

Figure 2.14 Slim-tube test data to determine MMP (Green and Willhite, 1998)

The other methods used to determine MMP are computational models include the equation of state (EOS) model and the analytical model[9]. This MMP is a strong function of temperature, composition of the crude oil system, and composition of the gas injection (Ahmad, 2000).

In this study, MMP values are taken from Hamouda et al., (2009), as shown in Figure 2.15. As can be seen in Figure 2.15, PVTSim data lie in the middle and it used in this study.

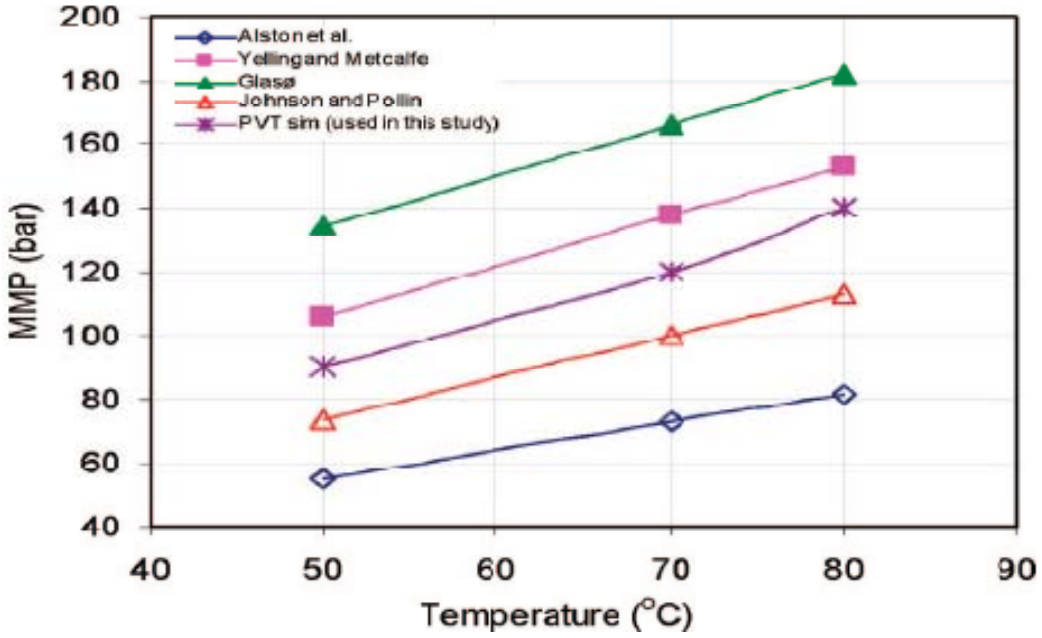

Figure 2.15 MMP values (bar) obtained from different empirical correlations and PVTSim for temperatures of 50, 70 and 80 °C (Hamouda et al., 2009)

3 EXPERIMENTAL SECTION

3.1 Material

3.1.1 Core samples

Core samples used in this experiment are outcrop chalks obtained from Stevns Klint, near Copenhagen in Dermark, with average porosity of 40-45%. The length of core samples varies from 0.78-1.19 cm with diameter 3.8 ± 0.001 cm. The chemical composition of Stevns Klint chalk is given in Table 3.1.

Table 3.1 Stevns Klint chalk chemical composition analysis (wt %) (Chukwudeme, 2009)

Si	Al	Mg	Ca
1.44	0.47	0.69	97.42

The characteristic properties of Stevns Klint chalk are as follow (Mirza, 2009):

- Age: Maastrichtian
- Average porosity: approximately 40-45%
- Silica content: less than 2%
- Absolute permeability: 3-5 mD
- Average pore throat size: 0.25 μm
- Median pore throat: 0.18- 0.35 μm
- The chalk is nearly homogenous

3.1.2 Oil phase

The oil sample used in this experiment is modified crude oils. This modified crude oil contains asphaltene, crude oil and toluene (0.25 g of asphaltene dissolved in 22 ml of toluene and mixed together with

100 ml of crude oil). The mixture is then equilibrated by using a magnet stirrer for at least 24 hours to ensure that all asphaltene are dissolve in the solution and then filtered through a 0.65 μm filter (Millipore). The chemical composition of modified crude oil is given in the Table 3.2.

Table 3.2 Modified crude oil chemical composition analysis (Ladsten, 2010)

Component	Weight %	Mole%
Nitrogen	0.00	0.00
Carbondioksid	0.00	0.00
C1, (P)	0.00	0.00
C2, (P)	0.00	0.00
C3, (P)	0.00	0.00
i-C4, (P)	0.00	0.00
n-C4, (P)	0.00	0.00
2,2-DM-C3 (P)	0.00	0.00
Ic5 (P)	0.00	0.00
nC5 (P)	0.00	0.00
Hexanes Total	0.00	0.00
Hexanes - P	0.00	0.00
Hexanes - N	0.00	0.00
Heptanes Total	0.10	0.12
Heptanes - P	0.09	0.10
Heptanes - N	0.01	0.02
Heptanes - A	0.00	0.00
Octanes Total	54.48	71.94
Octanes - P	0.15	0.16
Octanes - N	0.23	0.26
Octanes - A	54.10	71.52
Nonanes Total	0.56	0.54
Nonanes - P	0.32	0.30
Nonanes - N	0.20	0.20
Nonanes - A	0.04	0.04
Decanes Plus	44.86	27.40
Totals	100.00	100.00

Molecular weight of decanes plus (C_{10+}) is 199.47 g/mol, and density of modified crude oil is 0.87 g/ml.

3.2 Experimental procedure

3.2.1 Asphaltene preparation

In this experimental study, asphaltene is extracted from crude oil by using n-heptane as a solvent. Combination of 20 ml of crude oil and 800 ml of n-heptane (1:40) are mixed by magnet stirrer for at least 48 hrs until equilibrium is reached. The mixtures are then filtered through a 0.22 μm filter (Millipore). The filtration process is shown in Figure 3.1.

Figure 3.1 The filtration process of sample oil

After filtration process, the asphaltene must be dried using a vacuum drier at room temperature. The asphaltene must be dried properly for about 48 hours.

3.2.2 Core preparation

Outcrop chalk from Stevns Klint, near Copenhagen, Denmark is drilled with diameter of 3.9 ± 0.05 cm and dried in the oven at temperature of 120°C for at least 72 hours until a constant weight is obtained and the cores are totally dried. Then, the cores are cooled and shaved

using a lathe to diameter 3.8 ± 0.001 cm and cut to the desired length. The length of the core samples of ~1 cm are used to investigate the amount of precipitated asphaltene. With this short plug of ~1 cm (refer as core), faster experiment and more data can be obtained. The cores are then put under vacuum until pressure reach ~10^{-2} mbar before saturation process. A vacuum process of the core samples is shown in Figure 3.2.

Figure 3.2 A vacuum process of core samples

3.2.3 Core saturation

The cores are saturated under vacuum condition by the fluids used in this experiment (modified crude oil). After saturation process, the weight of cores is measured, and their pore volume and porosities are calculated by weight difference, bulk volume and fluid density using equation 3.1 and equation 3.2, respectively.

$$PV = \frac{W_{sat} - W_{dry}}{\rho_l} \tag{3.1}$$

$$\Phi = 100\ \frac{PV}{V_b} \tag{3.2}$$

Where:

PV = pore volume of core (cm^3)

V_b = bulk volume of core (cm^3)

W_{sat} = saturated weight of core (g)

W_{dry} = dried weight of core (g)

Φ = core porosity (%)

ρ_l = density of saturated liquid (g/cm^3).

Noted that the weight of the core must be measured immediately after the core is taken out of the oven to avoid any weight incremental caused by air humidity.

3.2.4 Core Aging

After the saturation process, the cores are then put inside the aging cell and fill it with the same fluid that was used for saturation process. The core must be aged for at least two weeks at temperature of 50°C, and then the CO_2 flooding process can be applied. The purpose of the aging of the core is to equilibrate the polar component of the oil with the core (rock). So, after aging process, we expect the core become an oil wet.

3.2.5 CO_2 flooding

After core aging for at least two weeks, the core is then ready for CO_2 flooding. The experimental setup used for the CO_2 flooding is shown in

Figure 3.3. The major components of this setup consist of a core holder, pressure regulator, gas flow meter, Gilson pump, piston cell and PC control Labview (version 7.1) to monitor and log the flooding data continuously.

Core saturated with modified crude oil is inserted into a core holder that consists of steel cylindrical body and rubber / Teflon sleeve. The confining pressure is applied on the sleeve and must be approximately 20 bar above the injection pressure. The required temperature is set by heat up the system using the oven.

In this experimental study, miscible CO_2 injection is applied to investigate the asphaltene precipitation. Pure CO_2 (99% purity) is injected from a piston cell via a Coriolis flow meter that records the inflow properties of CO_2 (mass flow rate and total mass injected). A back pressure regulator is installed downstream of the core to control the pressure difference between inlet and outlet of the core during CO_2 flooding. The pressure drop across the core is kept constant. The produced fluid from the core is collected in measuring glass.

CO_2 injection stopped when there is no oil production (at least 3 pore volumes). The pressure is decreased gradually and carefully controlled the overburden pressure (confine pressure) and the core pressure. The core can be removed from the core holder when the overburden pressure and the core pressure show zero bar.

The core is dried using the oven under vacuum condition at temperature of 120^{o}C. In order to increase the surface area exposed to the heat, the core is then crushed and dried again until a constant weight is obtained. A difference between the stable weight of the dried core and the stable weight of the crushed core about 0.5% is

obtained. The amount of asphaltene precipitation is calculated using mass balance of the dried core before saturation process and after CO_2 flooding.

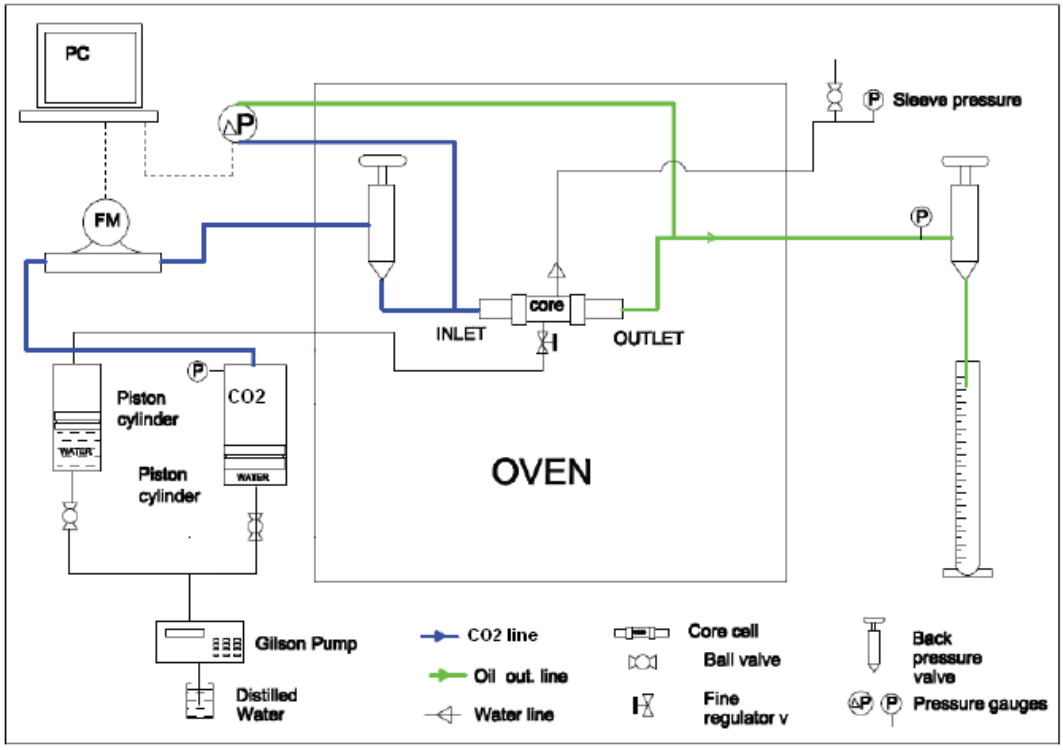

Figure 3.3 Schematic flow diagram of CO_2 flooding

3.2.6 Refractive index measurements

Refractive index is measured to confirm the precipitation of asphaltene in the core. This is done by measuring refractive index of the sample oil before and after CO_2 flooding using Abbe Refractometer (Carl Zeiss model). There is a different between the measured initial refractive index of the sample oil and the effluent after CO_2 flooding. The refractive index range is from 1.3000 to 1.7000.

4 RESULTS AND DISCUSSION

4.1 Model description

A thermodynamic model can be used to describe the behavior of asphaltene precipitation due to changes in pressure, temperature or composition (Hirschberg et al., 1984). One of the model input is asphaltene solubility properties. The solubility properties are pressure dependence. Decrease of pressure above bubble point will decrease the asphaltene solubility. Decrease of pressure below bubble point will increase the asphaltene solubility. Asphaltene solubility also decreases as a result of gas injection which is being dissolved in the crude oil.

Hirshberg et al., (1984) suggested a simplified model for the maximum volume fraction of the dissolved asphaltene in the crude oil:

$$(\emptyset_a)_{max} = exp\left[\frac{V_a}{V_L} - 1 - \frac{V_a}{RT}(\delta_a - \delta_L)^2\right] \quad (4.1)$$

Where:

$(\emptyset_a)_{max}$ = maximum volume fraction of the dissolved asphaltene in the crude oil

V_a = molar volume of asphaltene

V_L = molar volume of liquid phase

R = universal gas constant

T = temperature

δ_a = solubility parameter of asphaltene

δ_L = solubility parameter of liquid phase

Weight fraction of asphaltene precipitated is calculated by:

$$W_{Fa} = \frac{W_a}{W_{TL}} = \frac{W_{TaL} - W_{aL}}{W_{TL}} \tag{4.2}$$

Where:

W_{Fa}= weight fraction of asphaltene precipitated

W_a = weight of asphaltene precipitated

W_{TL}= total liquid weight

W_{TaL}= maximum weight of asphaltene in the liquid

W_{aL} = weight of asphaltene remaining in the liquid phase after flooding

The dissolved volume fraction of asphaltene in the liquid (V_{aL}) is given by equation 4.3:

$$V_{aL} = \frac{V_{TL} - \frac{W_{TL} - W_{aL}}{\rho_a}}{V_{TL}} \tag{4.3}$$

And volume fraction of precipitated asphaltene V_{Fa} is given by equation 4.4:

$$V_{Fa} = \frac{V_a}{V_{TL}} = \frac{\frac{W_a}{\rho_a}}{\frac{W_{TL}}{\rho_{TL}}} = \frac{W_a}{W_{TL}}\left(\frac{\rho_L}{\rho_a}\right) = W_{Fa}\left(\frac{\rho_L}{\rho_a}\right) \tag{4.4}$$

Where: V_{TL} and V_a are total volume of liquid and volume of precipitated asphaltene, respectively. ρ_L and ρ_a are density of liquid and asphaltene, respectively. W_{aL} is weight of asphaltene remain in the liquid.

The total weight of liquid W_{TL} is defined by re-written equation 4.3:

$$W_{TL} = (V_{TL} - V_{TL} * V_{aL})\rho_a + W_{aL} \quad (4.5)$$

By combining equation 4.2 and equation 4.5, the weight percent of precipitated asphaltene can be estimated by:

$$W_a(\%) = \frac{W_{TaL} - W_{aL}}{(V_{TL} - V_{TL} * V_{aL})\rho_a + W_{aL}} * 100 \quad (4.6)$$

In term of solubility parameters, the weight of asphaltene precipitation $W_a(\%)$ is given by equation 4.7:

$$W_a(\%) = \frac{W_{TaL} - W_{aL}}{\left[\mathrm{V_{TL}} - \mathrm{V_{TL}} * \exp\left(\frac{\mathrm{V_a}}{\mathrm{V_L}} - 1 - \frac{\mathrm{V_a}}{\mathrm{RT}}(\delta_a - \delta_L)^2\right)\right]\rho_a + W_{aL}} * 100 \quad (4.7)$$

Where:

W_{TaL} = total amount of asphaltene in the liquid (gr)

W_{aL} = weight of asphaltene in the liquid phase after flooding (gr)

V_{TL} = total volume of liquid (cm^3)

V_a = molar volume of asphaltene (cm^3/mol)

V_L = molar volume of liquid phase (cm^3/mol)

R = universal gas constant (8.31447 $Mpa.cm^3.mol^{-1}.K^{-1}$)

T = temperature (K)

δ_a = solubility parameter of asphaltene ($Mpa^{1/2}$)

δ_L = solubility parameter of liquid ($Mpa^{1/2}$)

ρ_a = density of asphaltene (gr/cm^3)

In this study, the density of asphaltene is taken as constant value of 1.28 g/cc refers to Parkash et al., (1979). Hirschberg et al., (1984) defined the solubility parameter of asphaltene as a function of temperature and given in equation 4.8:

$$\delta_a = 20.04[1 - 1.07 * 10^{-3} * T(C)] \quad (4.8)$$

The solubility parameter of liquid is given by equation 4.9[11]:

$$\delta_L = 16.581 \exp\left[-\beta * \frac{V_{CO_2}}{V_L}\right] \quad (4.9)$$

Where:

V_{CO_2} = molar volume of the CO_2 (cm^3/mol)

V_L = molar volume of liquid (cm^3/mol)

β = constant between 0.20-0.32

Substituting equation 4.8 and equation 4.9 into equation 4.7:

$$W_a(\%) = \frac{W_{TaL} - W_{aL}}{\left[V_{TL} - V_{TL} * \exp\left(\frac{V_a}{V_L} - 1 - \frac{V_a}{RT}\left(\delta_a - 16.581\exp\left[-\beta * \frac{V_{CO_2}}{V_L}\right]\right)^2\right)\right]\rho_a + W_{aL}} * 100 \quad (4.10)$$

Equation 4.10 is used in this study to calculate the weight percent of asphaltene precipitation in the core due to combined effects of pressure, temperature and CO_2.

4.2 Asphaltene precipitation

As mentioned before, three major factors affecting asphaltene precipitation are pressure, temperature, and compositional change of the crude oil. In this experiment, we found that constant pressure drop across the core also has a big effect on asphaltene precipitation. This thesis investigates the effect of pressure, temperature and constant pressure drop across the core on asphaltene precipitation.

4.2.1 Effect of pressure (flowing pressure)

Three different flowing pressure (90, 100, and 110 bar) are investigated with the same temperature of 50°C. The experimental asphaltene precipitation results predicted by the difference between initial and final weight of dried core is compared with the estimated results (using equation 4.10). Figure 4.1, Figure 4.2 and Figure 4.3 show the weight percent of asphaltene precipitation for pressure drop across the core of 1, 2 and 4 bar, respectively. It is noted that all experimental results give higher amount of asphaltene precipitation than estimated results. The deviation between experimental and estimated results is about ~22%.

It is interesting to see a consistent deviation of ~22% almost in all of the obtained results, where higher values are obtained from the experiments. This may be explained based on experimental error that may account for about 4% due to incomplete dryness of the core and experimental handling. The rest of the deviation value may be explained by the applied equation. The used equation is developed based on the best fit of the detailed compositional literature data (Hamouda et al., 2009). There is always uncertainty regarding the molecular weight of the asphaltene. In the work, the molecular weight of the asphaltene is taken as 1000. Span of reported molecular weight goes from about 500 to over 1000. The reported experimental data are based on injected CO_2, which then has to be recombined at different reported conditions of temperature and pressures, hence using asphaletene molecular weight of 1000. This process is followed (Hamouda et al., 2009) prior to taken the best fit. It is believed that this has contributed further to the error, with evidence of the error consistency.

Both experimental and estimated results show that the maximum amount of asphaltene precipitation occurs at pressure of 100 bar. In this study, at temperature of 50°C, the bubble point pressure is around 100 bar (phase envelope shown in Appendix). Above or below bubble point pressure, the amount of asphaltene precipitation is reduced.

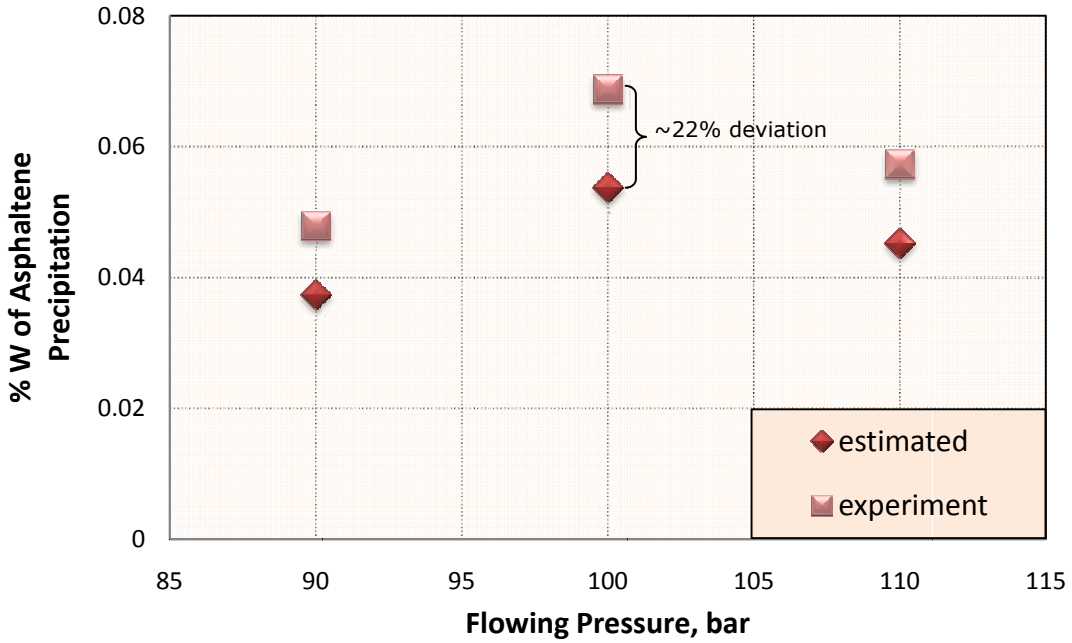

Figure 4.1 Weight percent of asphaltene precipitation as a function of flowing pressure at temperature of 50°C and pressure drop across the core of 1 bar

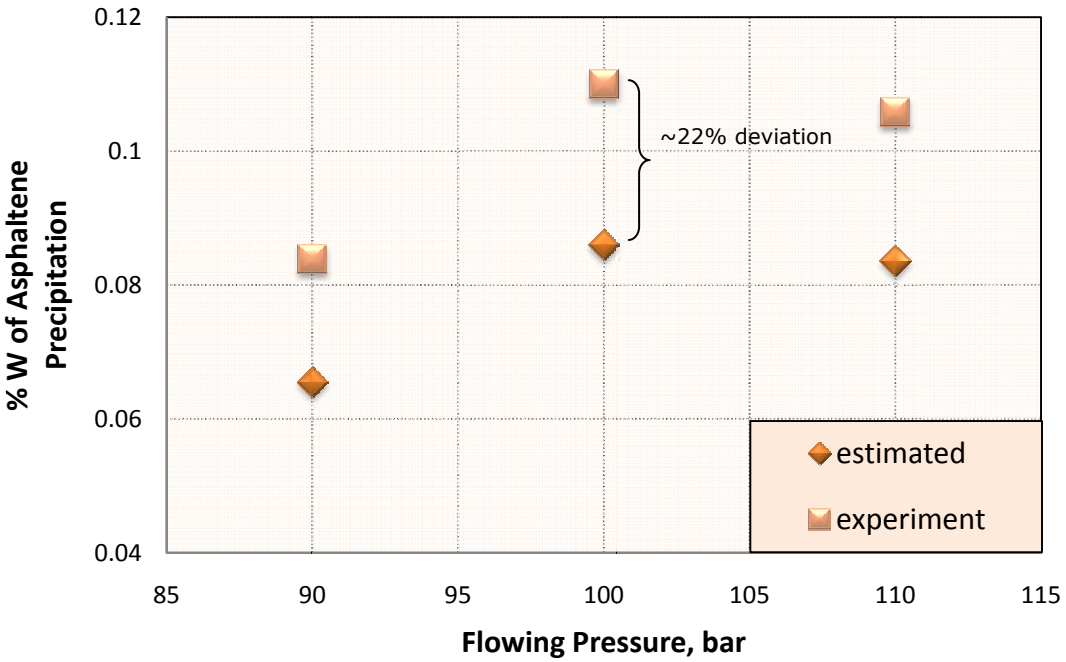

Figure 4.2 Weight percent of asphaltene precipitation as a function of flowing pressure at temperature of 50°C and pressure drop across the core of 2 bar

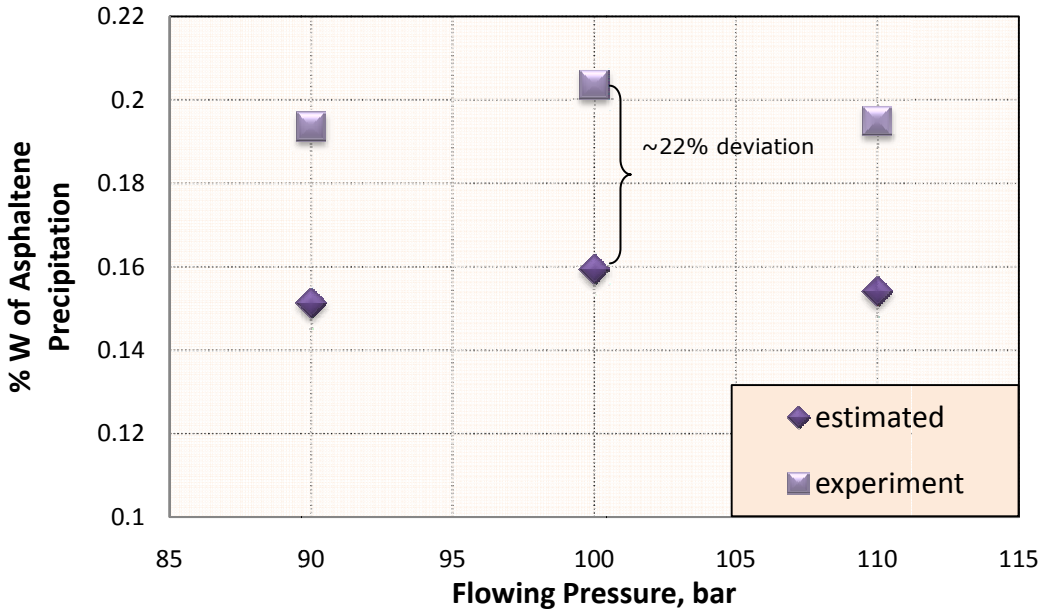

Figure 4.3 Weight percent of asphaltene precipitation as a function of flowing pressure at temperature of 50°C and pressure drop across the core of 4 bar

Moqadam et al., (2009) explained this phenomenon by density and solubility difference of oil and asphaltene suspension. When the pressure of the oil above bubble point decreases, its density and solubility parameter also decreases. This causes solubility difference between asphaltene and oil increases, assuming that asphaltene solubility parameter is manly function of temperature, which leads to asphaltene precipitation. When the pressure below the bubble point decreases, the light component is released from the oil to become free gas, consequently the solubility of the asphaltene in oil increases. This causes some of precipitated / suspended asphaltene to re-dissolved back into the oil.

The effect of pressure on asphaltene precipitation also can be explained by P-T diagram or asphaltene phase envelope (Figure 2.6) (Schlumberger Oil Field Review Summer, 2007). During primary depletion, the asphaltene start to precipitate when the pressure reaches the upper asphaltene-precipitation envelope. The precipitation increases as the pressure decreases and reaches a maximum at the bubble point pressure. As pressure continue to decrease, some of gas is released from the oil and the oil starts to re-dissolved asphaltene at the lower asphaltene-precipitation envelope.

4.2.2 Effect of temperature

The next parameter that has been investigated in this study is flowing temperature. Three different flowing temperatures (30, 40 and 50^{o}C) are investigated with the same pressure of 100 bar. The amount of precipitated asphaltene from experimental results and estimated (using equation 4.10) for pressure drop across the core of 1 bar are shown in Figure 4.4. In this investigation, the amount of precipitated

asphaltene from the experiment is also higher than estimated results. As explained previously the reason for higher experimental results than the estimated results is due to incomplete drying process of the core after CO_2 flooding.

It is shown that asphaltene precipitation increase with temperature. The maximum precipitated asphaltene occurs at 50°C (near bubble point).

The same trends are shown for pressure drop across the core of 2 and 4 bar. Figure 4.5 and Figure 4.6 illustrate the amount of precipitated asphaltene for pressure drop across the core of 2 and 4 bar, respectively.

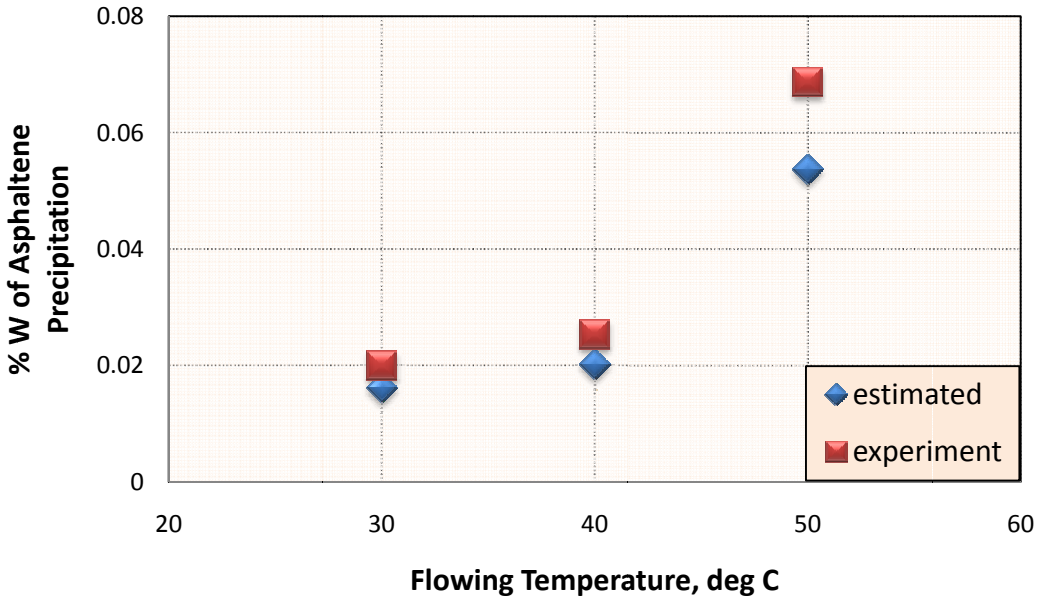

Figure 4.4 Weight percent of asphaltene precipitation as a function of temperature at pressure of 100 bar and pressure drop across the core of 1 bar

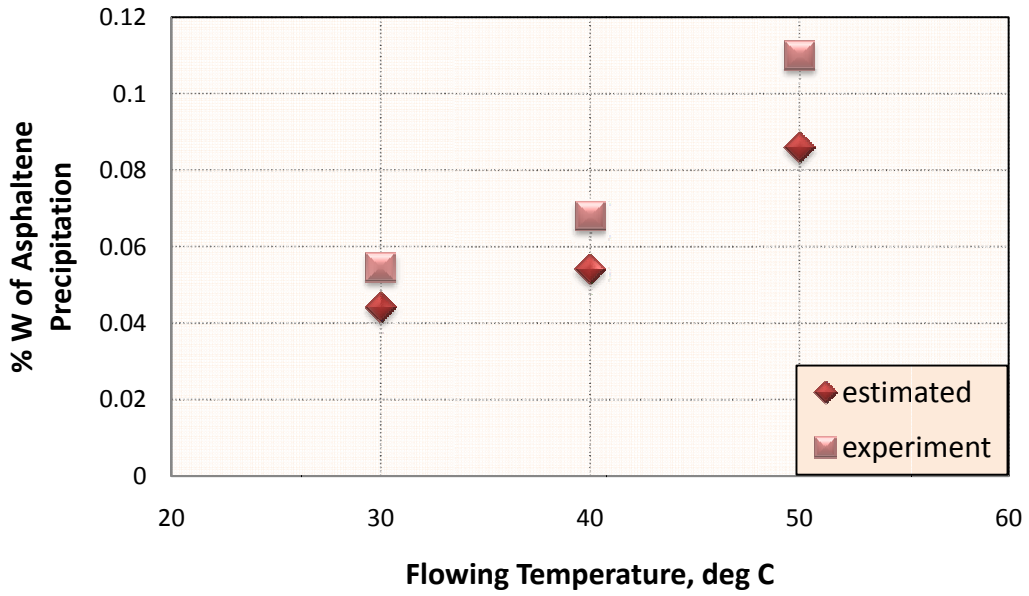

Figure 4.5 Weight percent of asphaltene precipitation as a function of temperature at pressure of 100 bar and pressure drop across the core of 2 bar

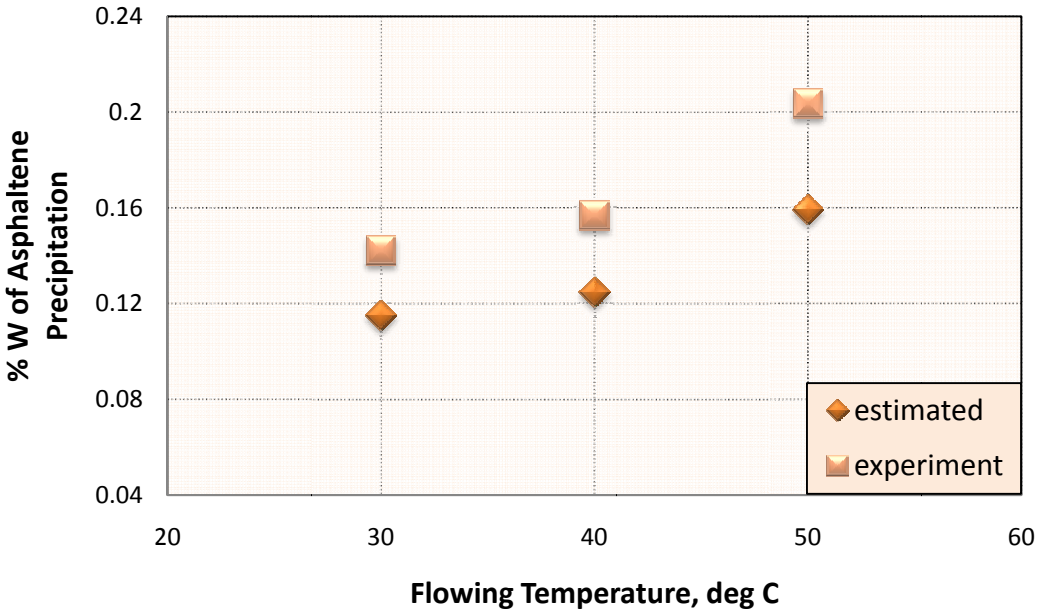

Figure 4.6 Weight percent of asphaltene precipitation as a function of temperature at pressure of 100 bar and pressure drop across the core of 4 bar

Escrochi et al., (2008) reported that the amount of asphaltene precipitation would increase by increasing the temperature until the maximum amount reaches at bubble point, as shown in Figure 4.7. At temperature higher than the bubble point, asphaltene precipitation decreases. This is explained by the solubility of asphaltene in oil. It is shown that asphaltene solubility in oil would decrease by increasing temperature before the bubble point, which means more asphaltene precipitated. After the bubble point, the solubility of asphaltene in oil increases as the temperature increases, hence less asphaltene precipitation.

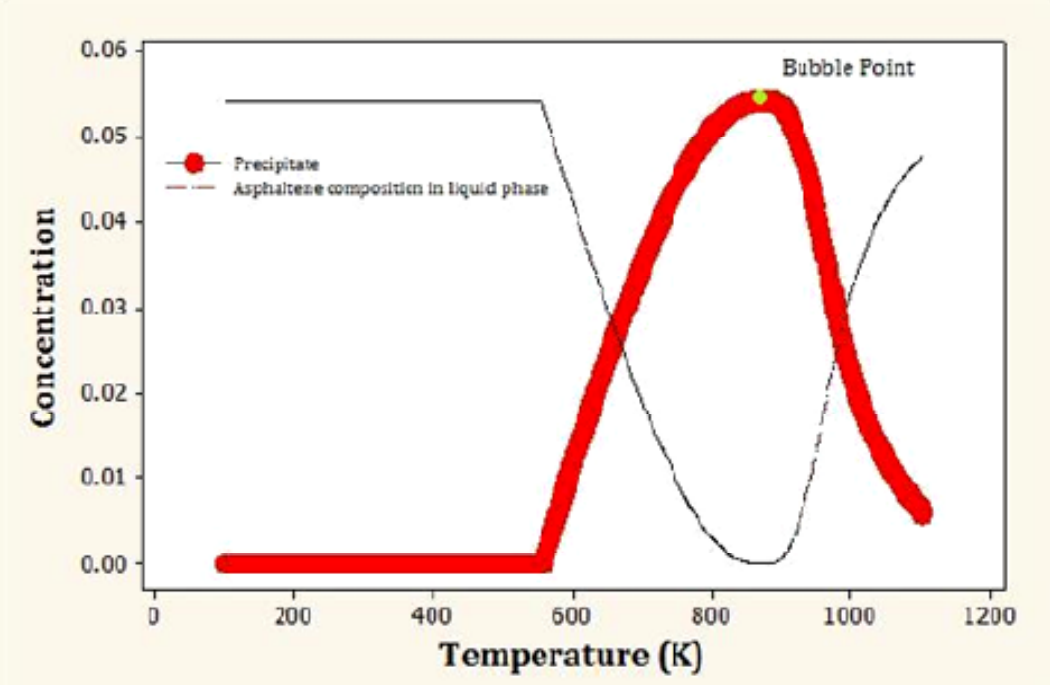

Figure 4.7 Asphaltene precipitation from Athabasca bitumen (Escrochi et al., 2008)

4.2.3 Effect of pressure drop

The effect of pressure drop across the core on asphaltene precipitation is the main subject of this study. Three different pressure drops (1, 2 and 4 bar) are investigated for three different pressures (90,100, and

110 bar) at 50^{0}C. The results are shown in Figure 4.8. As can be seen higher pressure drop gives higher asphaltene precipitation. Figure 4.8 also shows the effect of the flowing pressure changes on asphaltene precipitation. It is interesting to see that changes in pressure drop affect asphaltene precipitation, but not the flowing pressure. In other words, for the same pressure drop and different flowing pressure, the amount of asphaltene precipitation is almost the same.

Figure 4.8 also shows the maximum amount of asphaltene precipitation occurs at flowing pressure of 100 bar (near bubble point).

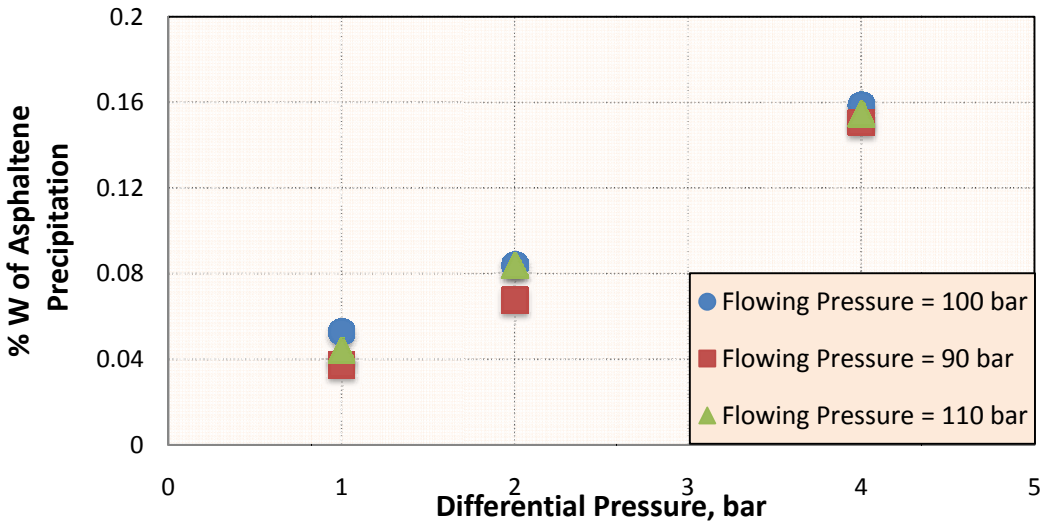

Figure 4.8 Weight percent of asphaltene precipitation as a function of pressure drop at flowing temperature of 50 ^{o}C

The same trends are shown for different flowing temperature. Figure 4.9 and Figure 4.10 illustrate the effect of pressure drop on asphaltene precipitation for temperature of 40^{o}C and 30^{o}C, respectively. Different with Figure 4.8, both Figure 4.9 and Figure 4.10 show that the maximum amount of asphaltene precipitation occurs at flowing pressure of 90 bar. The amount of asphaltene

precipitation decreases with the pressure. This is may be explained by phase envelope shown in Appendix. At temperature of 30 and 40°C, the pressure of 90 bar is close to bubble point.

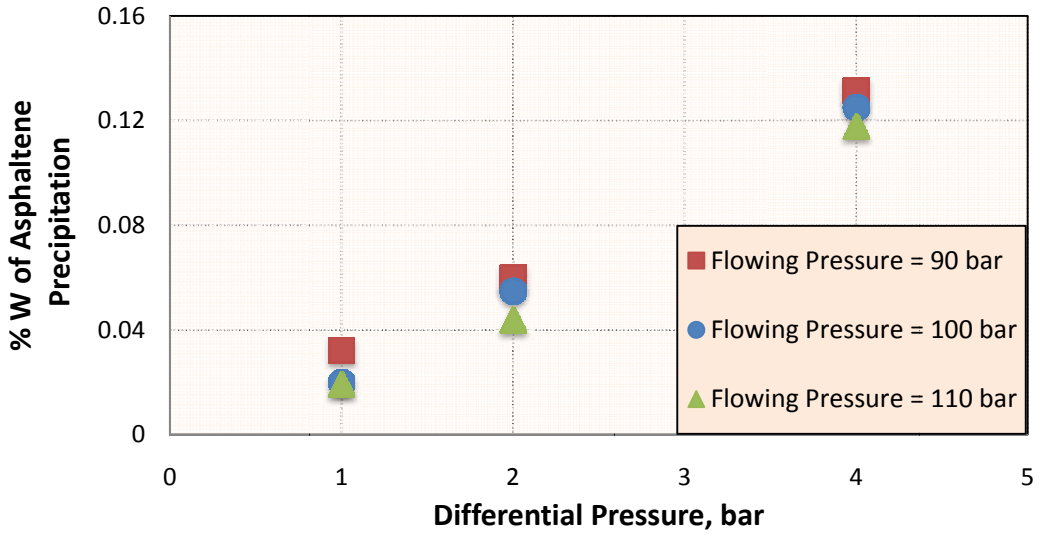

Figure 4.9 Weight percent of asphaltene precipitation as a function of pressure drop at flowing temperature of 40 °C

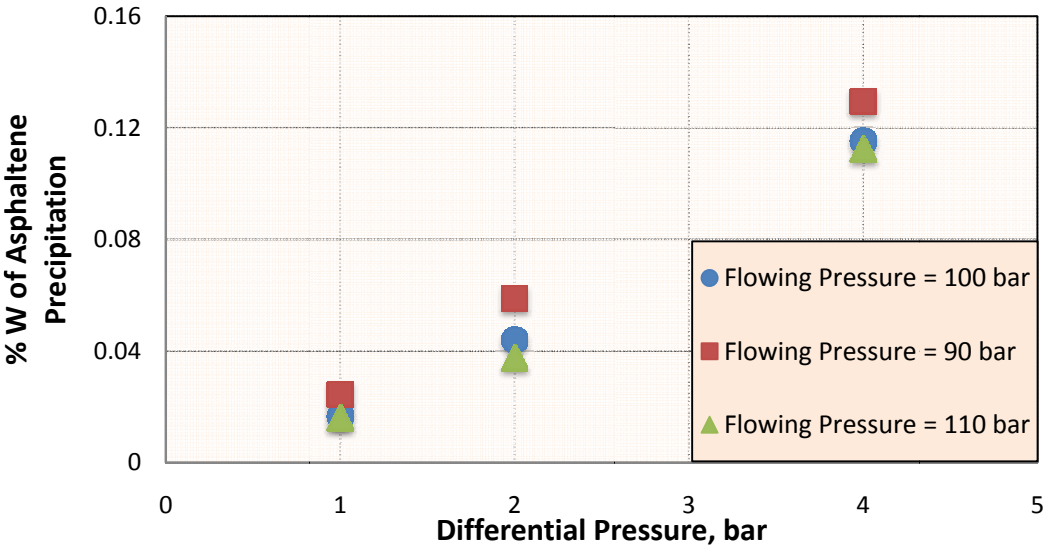

Figure 4.10 Weight percent of asphaltene precipitation as a function of pressure drop at flowing temperature of 30 °C

Chukwudeme and Hamouda, (2009) did experimental study about the effect of pressure drop across the core on asphaltene precipitation. The experiment is done using model oil (0.19-0.66 wt % asphaltene dissolved in toluene and 0.005M stearic acid (SA) dissolved in n-decane) without CO_2 injection, only contribution of pressure, temperature and CO_2 dissolved in the oil. The results are shown in Figure 4.11. It is clearly showing that the pressure drop affects the asphaltene precipitation, but not the flowing pressure. This may be explained by flow restrictions inside the core.

Thanyamanta et al., (2008) found that flow restrictions cause asphaltene to precipitate due to drastic change in conditions. In isothermal processes asphaltene started to precipitate somewhere inside the restriction. This means that the pressure drop induced by flow restriction was the main cause of asphaltene formation. In this study, higher pressure drop across the core causes higher restrictions, resulting higher asphaltene precipitation.

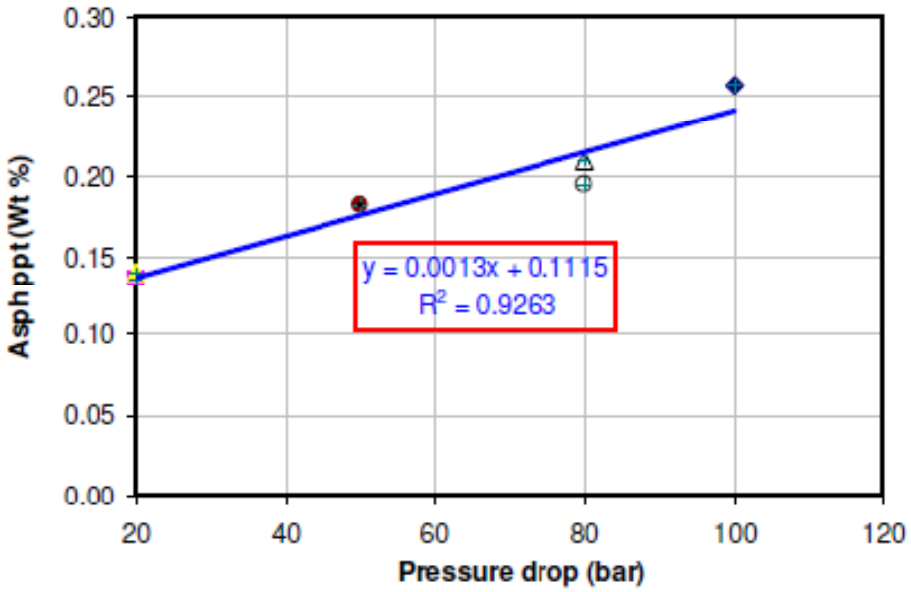

Figure 4.11 Asphaltene precipitation as a function of pressure drop at flowing temperature of 100 °C (Chukwudeme et al., 2009)

4.2.4 Refractive Index

In this study, refractive index (RI) is used to qualitatively confirm the asphaltene precipitation in the core. This is done by measuring the RI of the crude oil before and after CO_2 flooding. Delta RI qualitatively reflects the deposit asphaltene under the testing condition. The larger the difference between initial and final RI (delta RI), the larger the asphaltene precipitated.

Figure 4.12, Figure 4.13 and Figure 4.14 are the delta RI as a function of pressure drop for temperature of 50, 40 and 30^{o}C, respectively. As expected higher pressure drop across the core gives higher delta RI. Higher delta RI indicates higher asphaltene precipitated. This result is in agreement with the previous data where higher pressure drop across the core gives higher asphaltene precipitated.

Figure 4.12 shows the maximum delta RI occurs at flowing pressure of 100 bar. This result supports the previous data (Figure 4.8) where the maximum amount of asphaltene precipitation occurs at the pressure near to bubble point.

Figure 4.13 and Figure 4.14 show the maximum delta RI occurs at flowing pressure of 90 bar (near bubble point). These results also support the previous data (Figure 4.9 and Figure 4.10, respectively). So, it is clear that the maximum amount of asphaltene precipitation occurs at bubble point condition.

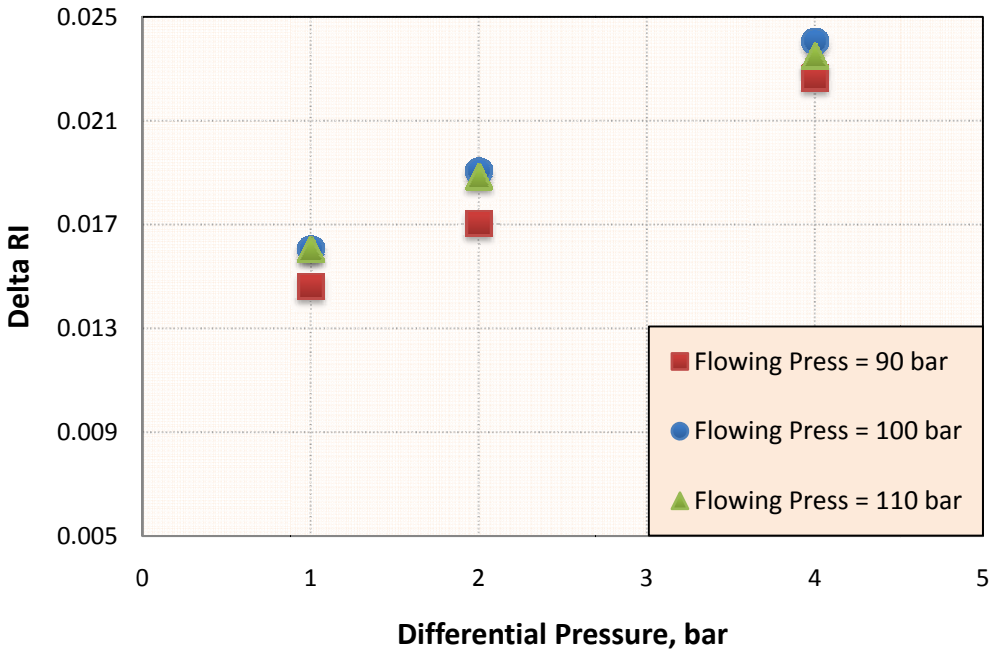

Figure 4.12 Delta RI as a function pressure drop for three different pressures and at temperature of 50°C

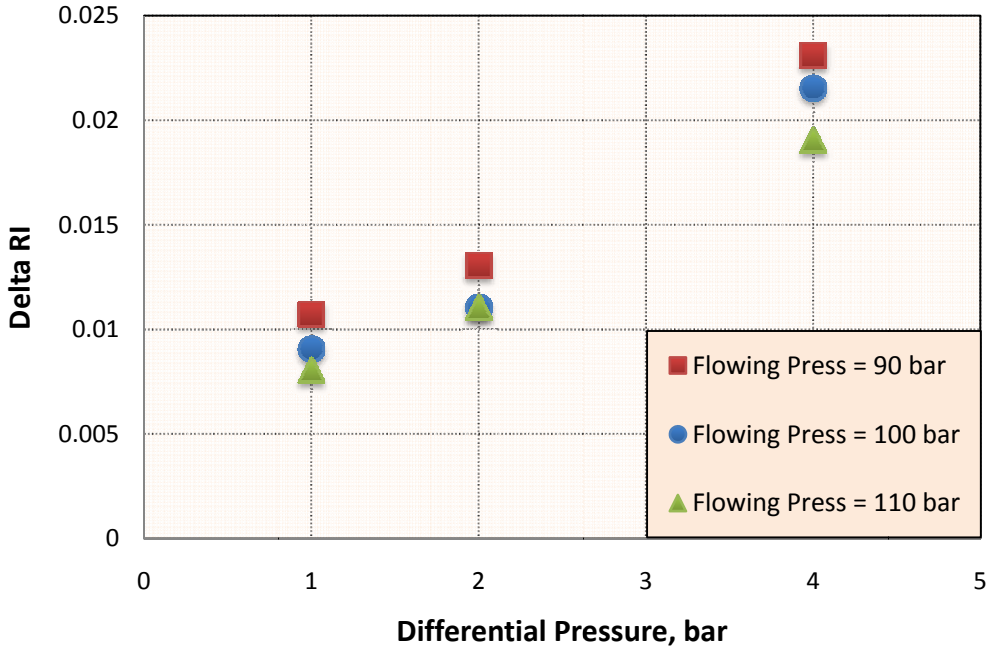

Figure 4.13 Delta RI as a function pressure drop for three different pressures and at temperature of 40°C

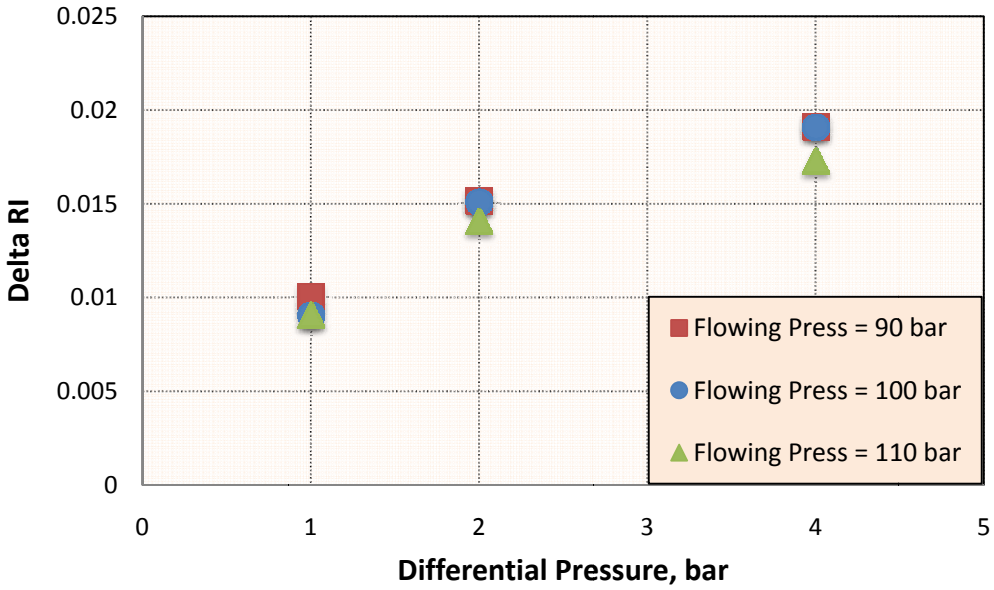

Figure 4.14 Delta RI as a function pressure drop for three different pressures and at temperature of 30°C

4.2.5 Effect of pressure drop without CO_2 injection

The effect of pressure drop on asphaltene precipitation without CO_2 injection (only contribution of pressure and temperature) is also investigated. The modified crude oil is used in this investigation. This is referred to work done by Chukwudeme et al., (2009) where model oil (0.19-0.66 wt % asphaltene dissolved in toluene and 0.005M stearic acid dissolved in n-decane) is used, as described in previous section (section 4.2.3, Figure 4.11). This result shows that pressure drop affects the asphaltene precipitation, but not the flowing pressure.

In this study, the experimental result to investigate the effect of pressure drop on asphaltene precipitation without CO_2 injection was not successful. This is suspected due to incomplete drying process. In this experiment, the drying process takes longer time than with CO_2 injection since higher volume of oil (modified crude oil) inside the core

after the experiment. In CO_2 injection, the drying process took about 3 weeks to dry the core, but in this experiment, the oil still remains in the core even after 6 weeks. And due to short time duration of this thesis, this data cannot be used. However, the delta RI can be used as qualitative data to investigate the amount of asphaltene precipitation inside the core.

Figure 4.15 show the delta RI as a function of pressure drop with and without CO_2 injection for pressure of 110 bar and at temperature of 50°C. As can be seen the CO_2 injection gives higher amount precipitation than pressure alone. The asphaltene precipitation increases when the CO_2 fraction in the fluid exceeds a critical point (Hamouda et al., 2009). Below the critical content, the precipitation of asphaltene is caused mainly by the pressure drop and temperature. Hamouda et al., (2009) also reported that the average critical content of about 33 mol % of CO_2 in the liquid. This study has an average mol % of CO_2 about 73%, which gives higher amount of asphaltene precipitation than without CO_2 injection (only pressure).

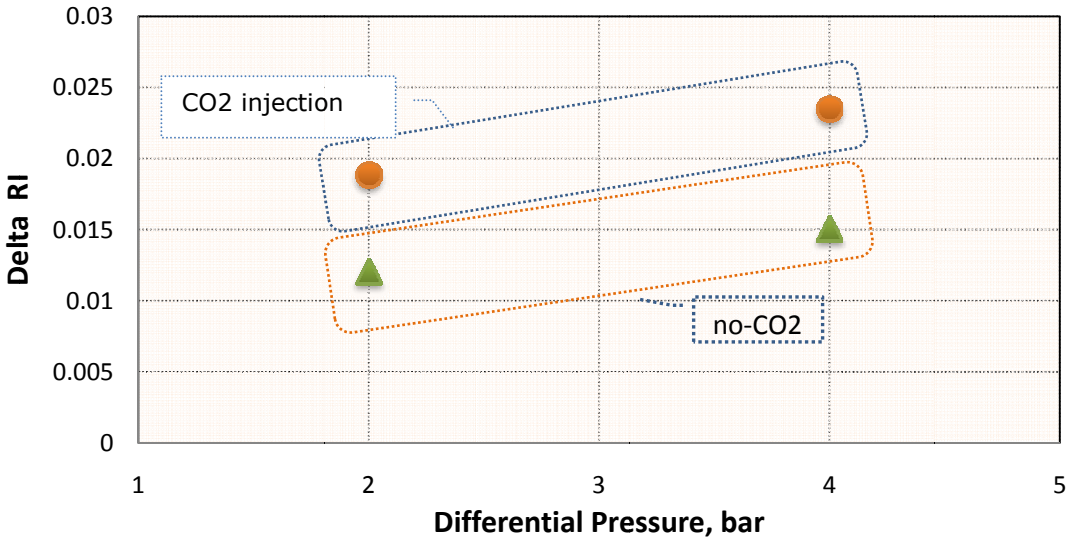

Figure 4.15 Delta RI as a function of pressure drop with and without CO_2 injection for pressure of 110 bar and at temperature of 50°C

Figure 4.16 shows a comparison between the experimental results done in this work and reported in literature, Chukwudeme and Hamouda, (2009). The experimental work results are done using modified crude oil with CO_2 injection and at temperature of 50°C. While the reported results, Chukwudeme and Hamouda (2009) used model oil without CO_2 injection and at temperature of 100°C.

The experimental result shows that increase in 1 bar of pressure drop gives 0.035% weight of asphaltene precipitation. Similar for Chukwudeme et al., (2009), increase in 1 bar of pressure drop gives 0.0013% weight of asphaltene precipitation. The difference between the experimental results and Chukwudeme and Hamouda (2009) may be explained based on the difference of condition during the experiment as described above.

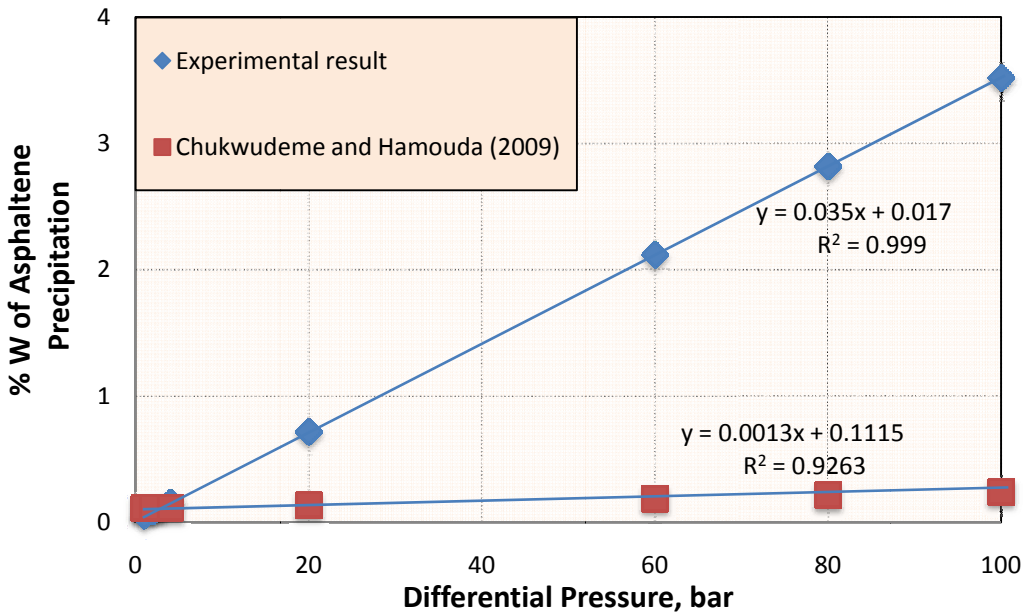

Figure 4.16 A Comparison between the experimental results and reported in literature, Chukwudeme and Hamouda, 2009

5 CONCLUSIONS

In this study, CO_2 is injected (at least 3 pore volumes until there is no oil production) to the core (saturated with modified crude oil) to investigate the effect of pressure, temperature and pressure drop across the core on asphaltene precipitation.

The experimental asphaltene precipitation results predicted by the difference between initial and final weight of dried core is compared with the estimated results (using equation 4.10). It is shown that experimental results give higher amount of precipitated asphaltene than estimated results. This may be explained based on incomplete drying process of the core after CO_2 flooding. The drying process took about 3 weeks under temperature of 120^{o}C and vacuum condition (pressure of 10^{-2} bar). It is suspected that the cores are not completely dry, hence higher amount of asphaltene precipitated obtained.

It is interesting to see a consistent deviation of ~22% almost in all of the obtained results, where higher values are obtained from the experiments. This may be explained based on experimental error (incomplete dryness of the core and experimental handling) and adjusted molecular weight of the asphaltene.

At a constant temperature (isothermal condition), the amount of asphaltene precipitation increases as the pressure decreases, and reaches the maximum at bubble point. As the pressure decreases, further the amount of asphaltene precipitation decreases. This is in agreement with literature where the maximum deposition occurs at the bubble point.

Similarly for constant flowing pressure, the amount of asphaltene precipitation increases with the temperature until the bubble point is reached.

It is shown in this work that the pressure drop affects the precipitation more than the pressure.

The difference in the refractive index between the inlet fluid and the outlet (delta RI) is used as a qualitative means to confirm the asphaltene precipitation in the core. This is done by measuring the refractive index of the crude oil before and after CO_2 flooding.

REFERENCES

1. Ahmad, T. 2000. Minimum Miscibility Pressure from EOS. Paper 2000-01 presented at the Petroleum Society's Canadian International Petroleum Conference held in Calgary, Alberta, Canada, 4-8 June.
2. Buckley, J.S., Hirasaki, G.J., Liu, Y., Drasek, S.V., Wang, J.X., Grill, G.S., 1998. Asphaltene Precipitation and Solvent Properties of Crude Oils. Petroleum Science and Technology (1998) 16, No. 3-4, p 251-285.
3. Chukwudeme, E., A., 2009. PhD Thesis – Investigating Factors Influenceing Recovery of Asphaltenic Oil by Water and Miscible CO_2 Flooding. University of Stavanger, Norway.
4. Chukwudeme, E.A., Hamouda, A. A., 2009. Enhanced Oil Recovery (EOR) by Miscible CO_2 and Water Flooding of Asphaltenic and Non-Asphaltenic Oils. Energies 2009, 2, p 714-737.
5. deBoer, R.B., Leerlooyer, K., Eigner, M.R.P., vanBergen, A.R.D., 1992. Screening of Crude Oil for Asphalt Precipitation: Theory, Practice, and the Selection of Inhibitors. Paper SPE 24987 presented at the European Petroleum Conference held in Cannes, 16-18 November.
6. Enhanced Oil Recovery Backgrounder – Gas Flooding. http://www.canopetro.com/technology.asp
7. Elsharkawy, A.M., Poettmann, F.H., Christiansen, R.L., 1996. Measuring CO_2 Minimum Miscibility Pressure: Slim-Tube or Rising-Bubble Method. Energy & Fuel 1996, 10, p 443-449.
8. Escrochi, M., Nabipour, M., Ayatollahi, S., Mehranbod, N., 2008. Wettability Alteration at Elevated Temperatures: The Consequences of Asphaltene Precipitation. Paper SPE 112428 presented at SPE International Symposium and Exhibition on

Formation Damage Control held in Lafayette, Louisiana, U.S.A., 13-15 February.

9. Green, D.W., Willhite, G.P., 1998. Enhanced Oil Recovery. SPE Text book Series Vol. 6.
10. Hamouda, A.A., Chukwudeme, E.A., Mirza, D., 2009. Investigating the Effect of CO_2 Flooding on Asphaltenic Oil Recovery and Reservoir Wettability. Energy & Fuel 2009. 23. P 1118-1127.
11. Hamouda, A.A., Chukwudeme, E.A., Tabrizy, V.A., 2010. Influence of Temperature on Water and CO_2 Flooding of Asphaltenic Chalk Reservoirs: Experimental and Simulation Case Study. Paper SPE 131190 presented at the SPE EUROPEC/EAGE Annual Conference and Exhibition held in Barcelona, Spain, 14-17 June.
12. Hirschberg, A., deJong, L.N.J., Schipper, B.A., Meijer, J.G., 1984. Influence of Temperature and Pressure on Asphaltene Flocculation. Society of Petroleum Engineering Journal, vol. 24, June: 283-293.
13. International Energy Agency – Oil Market Report, 12 April 2011.
14. Kokal, S.L., Sayegh, S.G., 1995. Asphaltene: The Cholesterol of Petroleum. Paper SPE 29787 presented at the SPE Middle East Oil Show held in Bahrain, 11-14 March.
15. Ladsten, S.V., 2010. Laboratorierapport – Komposisjon og Asfalten Analyser. Intertek West Lab. Norway.
16. Lei, H., Pingping, S., Ying, J., Jigen, Y., Shi, L., Aifang, B., 2010. Prediction of Asphaltene Precipitation during CO_2 Injection. Petroleum Exploration and Development, Volume 37, p 349-353.
17. Mansoori, G.A., 2005. Nanoscale Structures of Asphaltene Molecule, Asphaltene Steric –Colloid and Asphaltene Micelles & Vehichles, http://tigger.uic.edu/~mansoori/Asphaltene.Molecule_html.
18. Mansoori, G.A., 2010. Remediation of Asphaltene and Other Heavy Organic Deposits in Oil Wells and in Pipelines.

http://www.uic.edu/labs/trl/1.OnlineMaterials/10.Remediation_of_Asphaltene.SOCAR_JOURNAL.pdf

19. Metcalfe, R.S., 1982. Effects of Impurities on Minimum Miscibility Pressure and Minimum Enrichments Level for CO_2 and Rich-Gas Displacements. Society of Petroleum Engineering Journal, p 219-225.
20. Mirza, D., 2008. MSc. Thesis – CO_2 Injection of Enhanced Oil Recovery: Miscible Process. University of Stavanger, Norway.
21. Moqadam, M.S., Firoozinia, H., Kharrat, R., Ghazanfari, M.H., 2009. Effect of Pressure and CO2 Composition Changes on Distribution of Asphaltene Molecular Wieght in Heavy Crude Oil. Paper Petroleum Society 2009-037 presented at the Canadian International Petroleum Conference (CIPC), Calgary, Alberta, Canada, 16-18 June.
22. Negahban, S., Bahamaish, J.N.M, Joshi, N., Nighswander, J., Jamaluddin, A.K.M., 2004. An Experimental Study at an Abu Dhabi Reservoir of asphaltene Precipitation Caused by Gas Injection. Paper SPE 80261 presented at the SPE International Symposium on Oilfield Chemistry, Houston, 5-7 February.
23. Okwen, R.T., 2006. Formation Damage by CO_2-Induced Asphaltene Precipitation. Paper SPE 98180 presented at the International Symposium and Exhibition on Formation Damage Control held in Lafayette, LA, 15-17 February.
24. Oskui, G.P., Jumaa, M.A., 2009. Laboratory Investigation of Asphaltene Precipitation Problems during CO_2/hydrocarbon Injection Project for EPR Application in Kuwaiti Reservoirs. Paper SPE 126267 presented at Kuwait International Petroleum Conference and Exhibition held in Kuwait City, Kuwait, 14-16 December.

25. Parkash, S., Moschopedis, S., Speight, J., 1979. Physical Properties and Suface Characteristics of Asphaltenes. Fuel, 1979, 58, p 877 – 882.
26. Rathmell, J.J., Stalkup, F.I., Hassinger, R.C., 1971. A Laboratory Investigation of Miscible Displacement by Carbon Dioxide. Paper SPE 3483 presented at the 46th Annual Fall Meeting of the Society Petroleum Engineers of AIME held in New Orleands, La, 3-6 October.
27. Schlumberger Oil field Review Summer 2007. Asphaltenes – Problematic but Rich and Potential.
28. Takhar, S., Ravenscroft, P.D., Nicoll, D.C.A., 1995. Prediction of Asphaltene Deposition during Production – Model Description and Experimental Details. Paper SPE 30108 presented at the European Formation Damage Conference held in The Hague, The Netherlands, 15-16 May.
29. Thanyamanta, W., Johansen, T.E., Hawboldt, 2008. Prediction of Asphaltene Precipitation Using non-Isothermal Compositional Network Model. Journal of Petroleum Science and Engineering 64, p 11-19.
30. Wang, S., Civan, F., 2005. Preventing Asphaltene Deposition in Oil Reservoir by Early Water injection. Paper SPE 94268 presented at the SPE Production and Operations Symposium held in Oklahoma City, OK, U.S.A., 17-19 April.
31. Vafaie-Sefti, M., Mousavi-Dehghani, S.A., Mohamad-Zadeh, M., 2002. A Simple Model for Asphaltene Deposition in Petroleum Mixtures. Fluid Phase Equilibria PII: S0378-3812(02)00301-1.
32. Yin, Y.R., Yen, A.T., Asomaning, S., 2000. Asphaltene Inhibitor Evaluation in CO2 Floods: Laboratory Study and Field Testing. Paper SPE 59706 presented at Permian Basin Oil and Gas Recovery Conference held in Midland, Texas, 21-23 March.

33. Yongmao, H., Zenggui, W., Yueming, J.B.C., Xiangjie, L., Petro, X., 2004. Laboratory Investigation of CO_2 Flooding. Paper SPE 88883 presented at the 28th Annual SPE International Technical Conference and Exhibition in Abuja, Nigeria, 2-4 August.
34. Zekri, A.Y., Shedid, S.A., Almehaideb, R.A., 2009. Sulfur and Asphaltene Deposition during CO_2 Flooding of Carbonate Reservoirs. Paper SPE 118825 presented at Middle East Oil & Gas Show and Conference held in Bahrain International Exhibition Center, Kingdom of Bahrain, 15-18 March.

APPENDIX A: Phase Envelope of Recombine Oil by CO_2

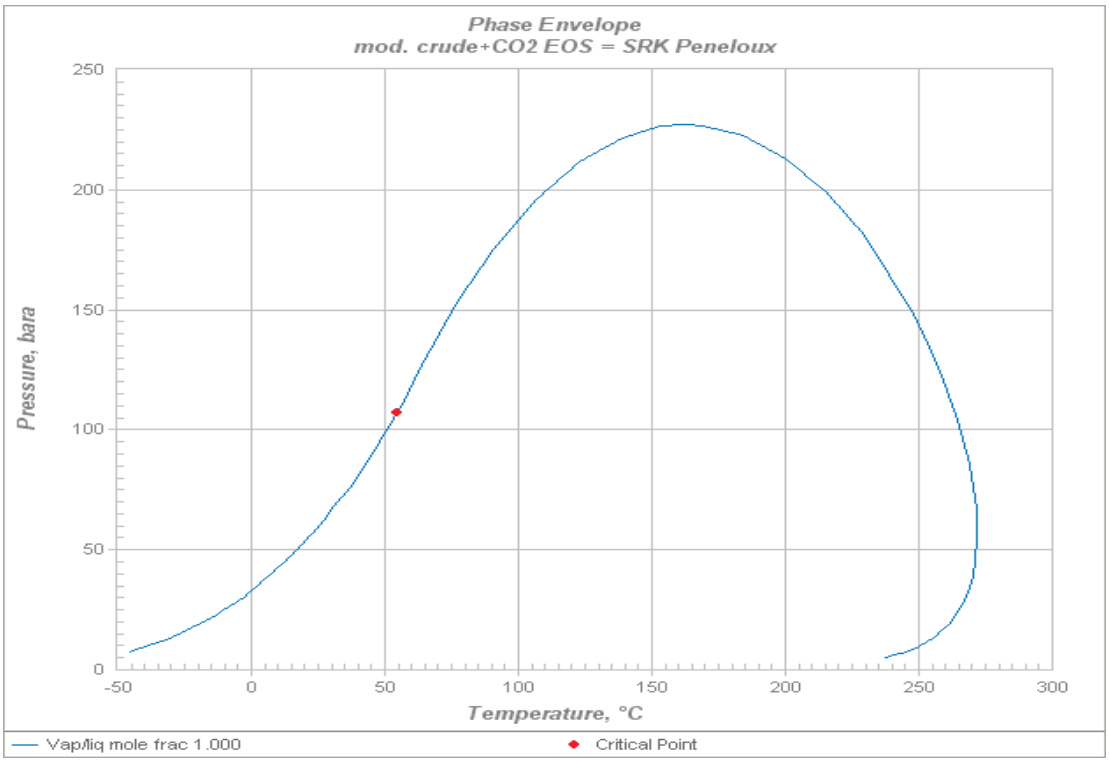

APPENDIX B: CO_2 Flooding Data and Calculation

Core data	:	Core 1
L(cm)	:	0.91
D(cm)	:	3.8
Area (cm2)	:	11.3426
Bulk volume(cc)	:	10.3205
Dry weight(g)	:	15.2836
Sat weight(g)	:	19.0900
PV(ml)	:	4.3911
Density of oil @15^{o}C(g/cc)	:	0.8668
Porosity (%)	:	43
Inject. Press(bar)	:	90
Confining press(bar)	:	110
Delta press (inlet – outlet) (bar)	:	1
Temp(^{o}C)	:	50
Refractive index before flooding	:	1.482770
Refractive index after flooding	:	1.468150
Delta Refractive Index	:	0.014620
Wt of asp. Inside the core before flooding (g)	:	0.0090
Wt of asp. Inside the core after flooding (g)	:	0.0021
Wt of asp. In the liquid after flooding (g)	:	0.0069
Total mass of CO_2 injected (g)	:	80
Mol % of CO_2	:	72.7
Wt of core after flooding and drying (g)	:	15.2857
Wt percent of precipitated asp. from experiment (%)	:	0.0478
Wt percent of precipitated asp. from calculation (%)	:	0.0373

APPENDIX B – Continued

Core data	:	Core 2
L(cm)	:	0.9
D(cm)	:	3.8
Area (cm2)	:	11.3426
Bulk volume(cc)	:	10.2071
Dry weight(g)	:	16.1247
Sat weight(g)	:	19.6400
PV(ml)	:	4.0553
Density of oil @15oC(g/cc)	:	0.8668
Porosity (%)	:	40
Inject. press(bar)	:	90
Confining press(bar)	:	110
Delta press (inlet - outlet) (bar)	:	2
Temp(°C)	:	50
Refractive index before flooding	:	1.482770
Refractive index after flooding	:	1.465725
Delta Refractive Index	:	0.017045
Wt of asp. inside the core before flooding (g)	:	0.0083
Wt of asp. inside the core after flooding (g)	:	0.0034
Wt of asp. In the liquid after flooding (g)	:	0.0049
Total mass of CO2 injected (g)	:	55
Mol % of CO2	:	72.7
Wt of core after flooding and drying (g)	:	16.1281
Wt percent of precipitated asp. from experiment (%)	:	0.08384081
Wt percent of precipitated asp. from calculation (%)	:	0.0654

APPENDIX B – Continued

Core data	:	Core 3
L(cm)	:	0.98
D(cm)	:	3.8
Area (cm2)	:	11.3426
Bulk volume(cc)	:	11.1144
Dry weight(g)	:	15.7046
Sat weight(g)	:	19.9600
PV(ml)	:	4.9091
Density of oil @15^{o}C(g/cc)	:	0.8668
Porosity (%)	:	44
Inject. press(bar)	:	90
Confining press(bar)	:	110
Delta press (inlet - outlet) (bar)	:	4
Temp(^{o}C)	:	50
Refractive index before flooding	:	1.482770
Refractive index after flooding	:	1.460125
Delta Refractive Index	:	0.022645
Wt of asp. inside the core before flooding (g)	:	0.0101
Wt of asp. inside the core after flooding (g)	:	0.0006
Wt of asp. In the liquid after flooding (g)	:	0.0095
Total mass of CO_2 injected (g)	:	85
Mol % of CO_2	:	72.7
Wt of core after flooding and drying (g)	:	15.7141
Wt percent of precipitated asp. from experiment (%)	:	0.193518353
Wt percent of precipitated asp. from calculation (%)	:	0.1512

APPENDIX B – Continued

Core data	:	Core 4
L(cm)	:	0.92
D(cm)	:	3.8
Area (cm2)	:	11.3426
Bulk volume(cc)	:	10.4339
Dry weight(g)	:	15.3888
Sat weight(g)	:	19.3000
PV(ml)	:	4.5120
Density of oil @15^{o}C(g/cc)	:	0.8668
Porosity (%)	:	43
Inject. press(bar)	:	100
Confining press(bar)	:	120
Delta press (inlet - outlet) (bar)	:	1
Temp(^{o}C)	:	50
Refractive index before flooding	:	1.482770
Refractive index after flooding	:	1.466715
Delta Refractive Index	:	0.016055
Wt of asp. inside the core before flooding (g)	:	0.0092
Wt of asp. inside the core after flooding (g)	:	0.0031
Wt of asp. In the liquid after flooding (g)	:	0.0061
Total mass of CO_2 injected (g)	:	85
Mol % of CO_2	:	72.8
Wt of core after flooding and drying (g)	:	15.3919
Wt percent of precipitated asp. from experiment (%)	:	0.0687
Wt percent of precipitated asp. from calculation (%)	:	0.0537

APPENDIX B – Continued

Core data	:	Core 5
L(cm)	:	0.89
D(cm)	:	3.8
Area (cm2)	:	11.3426
Bulk volume(cc)	:	10.0936
Dry weight(g)	:	15.8517
Sat weight(g)	:	19.3200
PV(ml)	:	4.0011
Density of oil @15^{o}C(g/cc)	:	0.8668
Porosity (%)	:	40
Inject. press(bar)	:	100
Confining press(bar)	:	120
Delta press (inlet - outlet) (bar)	:	2
Temp(^{o}C)	:	50
Refractive index before flooding	:	1.482770
Refractive index after flooding	:	1.463708
Delta Refractive Index	:	0.019062
Wt of asp. inside the core before flooding (g)	:	0.0082
Wt of asp. inside the core after flooding (g)	:	0.0044
Wt of asp. In the liquid after flooding (g)	:	0.0038
Total mass of CO_2 injected (g)	:	40
Mol % of CO_2	:	72.8
Wt of core after flooding and drying (g)	:	15.8561
Wt percent of precipitated asp. from experiment (%)	:	0.1100
Wt percent of precipitated asp. from calculation (%)	:	0.0860

APPENDIX B – Continued

Core data	:	Core 6
L(cm)	:	0.94
D(cm)	:	3.8
Area (cm2)	:	11.3426
Bulk volume(cc)	:	10.6607
Dry weight(g)	:	15.5924
Sat weight(g)	:	19.6800
PV(ml)	:	4.7155
Density of oil @15^{o}C(g/cc)	:	0.8668
Porosity (%)	:	44
Inject. press(bar)	:	100
Confining press(bar)	:	120
Delta press (inlet - outlet) (bar)	:	4
Temp(^{o}C)	:	50
Refractive index before flooding	:	1.482770
Refractive index after flooding	:	1.458710
Delta Refractive Index	:	0.024060
Wt of asp. inside the core before flooding (g)	:	0.0097
Wt of asp. inside the core after flooding (g)	:	0.0096
Wt of asp. In the liquid after flooding (g)	:	0.0001
Total mass of CO_2 injected (g)	:	70
Mol % of CO_2	:	72.8
Wt of core after flooding and drying (g)	:	15.6020
Wt percent of precipitated asp. from experiment (%)	:	0.2036
Wt percent of precipitated asp. from calculation (%)	:	0.1593

APPENDIX B – Continued

Core data	:	Core 7
L(cm)	:	0.9
D(cm)	:	3.8
Area (cm2)	:	11.3426
Bulk volume(cc)	:	10.2071
Dry weight(g)	:	14.9664
Sat weight(g)	:	19.7500
PV(ml)	:	5.5184
Density of oil @15^{o}C(g/cc)	:	0.8668
Porosity (%)	:	54
Inject. press(bar)	:	110
Confining press(bar)	:	130
Delta press (inlet - outlet) (bar)	:	1
Temp(^{o}C)	:	50
Refractive index before flooding	:	1.482770
Refractive index after flooding	:	1.466725
Delta Refractive Index	:	0.016045
Wt of asp. inside the core before flooding (g)	:	0.0089
Wt of asp. inside the core after flooding (g)	:	0.0025
Wt of asp. In the liquid after flooding (g)	:	0.0064
Total mass of CO_2 injected (g)	:	86
Mol % of CO_2	:	72.9
Wt of core after flooding and drying (g)	:	14.9689
Wt percent of precipitated asp. from experiment (%)	:	0.0573
Wt percent of precipitated asp. from calculation (%)	:	0.0452

APPENDIX B – Continued

Core data	:	Core 8
L(cm)	:	0.78
D(cm)	:	3.8
Area (cm2)	:	11.3426
Bulk volume(cc)	:	8.8461
Dry weight(g)	:	12.8557
Sat weight(g)	:	16.2300
PV(ml)	:	3.8926
Density of oil @15^{o}C(g/cc)	:	0.8668
Porosity (%)	:	44
Inject. press(bar)	:	90
Confining press(bar)	:	110
Delta press (inlet - outlet) (bar)	:	2
Temp(^{o}C)	:	40
Refractive index before flooding	:	1.482770
Refractive index after flooding	:	1.469715
Delta Refractive Index	:	0.013055
Wt of asp. inside the core before flooding (g)	:	0.0089
Wt of asp. inside the core after flooding (g)	:	0.0046
Wt of asp. In the liquid after flooding (g)	:	0.0043
Total mass of CO_2 injected (g)	:	81
Mol % of CO_2	:	72.9
Wt of core after flooding and drying (g)	:	14.5963
Wt percent of precipitated asp. from experiment (%)	:	0.1058
Wt percent of precipitated asp. from calculation (%)	:	0.0835

APPENDIX B – Continued

Core data	:	Core 9
L(cm)	:	0.87
D(cm)	:	3.8
Area (cm2)	:	11.3426
Bulk volume(cc)	:	9.8668
Dry weight(g)	:	14.1391
Sat weight(g)	:	17.9200
PV(ml)	:	4.3617
Density of oil @15^{o}C(g/cc)	:	0.8668
Porosity (%)	:	44
Inject. press(bar)	:	110
Confining press(bar)	:	130
Delta press (inlet - outlet) (bar)	:	4
Temp(^{o}C)	:	50
Refractive index before flooding	:	1.482770
Refractive index after flooding	:	1.459285
Delta Refractive Index	:	0.023485
Wt of asp. inside the core before flooding (g)	:	0.0089
Wt of asp. inside the core after flooding (g)	:	0.0085
Wt of asp. In the liquid after flooding (g)	:	0.0004
Total mass of CO_2 injected (g)	:	103
Mol % of CO_2	:	72.9
Wt of core after flooding and drying (g)	:	14.1476
Wt percent of precipitated asp. from experiment (%)	:	0.1949
Wt percent of precipitated asp. from calculation (%)	:	0.1540

APPENDIX B – Continued

Core data	:	Core 10
L(cm)	:	0.85
D(cm)	:	3.8
Area (cm2)	:	11.3426
Bulk volume(cc)	:	9.6400
Dry weight(g)	:	14.1373
Sat weight(g)	:	17.7900
PV(ml)	:	4.2138
Density of oil @15^{o}C(g/cc)	:	0.8668
Porosity (%)	:	44
Inject. press(bar)	:	90
Confining press(bar)	:	110
Delta press (inlet - outlet) (bar)	:	1
Temp(^{o}C)	:	40
Refractive index before flooding	:	1.482770
Refractive index after flooding	:	1.472050
Delta Refractive Index	:	0.010720
Wt of asp. inside the core before flooding (g)	:	0.0086
Wt of asp. inside the core after flooding (g)	:	0.0018
Wt of asp. In the liquid after flooding (g)	:	0.0068
Total mass of CO_2 injected (g)	:	54
Mol % of CO_2	:	73.3
Wt of core after flooding and drying (g)	:	14.1391
Wt percent of precipitated asp. from experiment (%)	:	0.0427
Wt percent of precipitated asp. from calculation (%)	:	0.0334

APPENDIX B – Continued

Core data	:	Core 11
L(cm)	:	0.78
D(cm)	:	3.8
Area (cm2)	:	11.3426
Bulk volume(cc)	:	8.8461
Dry weight(g)	:	12.8557
Sat weight(g)	:	16.2300
PV(ml)	:	3.8926
Density of oil @15^{o}C(g/cc)	:	0.8668
Porosity (%)	:	44
Inject. press(bar)	:	90
Confining press(bar)	:	110
Delta press (inlet - outlet) (bar)	:	2
Temp(^{o}C)	:	40
Refractive index before flooding	:	1.482770
Refractive index after flooding	:	1.469715
Delta Refractive Index	:	0.013055
Wt of asp. inside the core before flooding (g)	:	0.0080
Wt of asp. inside the core after flooding (g)	:	0.0029
Wt of asp. In the liquid after flooding (g)	:	0.0051
Total mass of CO_2 injected (g)	:	81
Mol % of CO_2	:	73.3
Wt of core after flooding and drying (g)	:	12.8586
Wt percent of precipitated asp. from experiment (%)	:	0.0745
Wt percent of precipitated asp. from calculation (%)	:	0.0583

APPENDIX B – Continued

Core data	:	Core 12
L(cm)	:	0.89
D(cm)	:	3.8
Area (cm2)	:	11.3426
Bulk volume(cc)	:	10.0936
Dry weight(g)	:	15.2952
Sat weight(g)	:	19.0100
PV(ml)	:	4.2855
Density of oil @15^{o}C(g/cc)	:	0.8668
Porosity (%)	:	42
Inject. press(bar)	:	90
Confining press(bar)	:	110
Delta press (inlet - outlet) (bar)	:	4
Temp(^{o}C)	:	40
Refractive index before flooding	:	1.482770
Refractive index after flooding	:	1.459675
Delta Refractive Index	:	0.0231
Wt of asp. inside the core before flooding (g)	:	0.0088
Wt of asp. inside the core after flooding (g)	:	0.0072
Wt of asp. In the liquid after flooding (g)	:	0.0016
Total mass of CO_2 injected (g)	:	91
Mol % of CO_2	:	73.3
Wt of core after flooding and drying (g)	:	15.3024
Wt percent of precipitated asp. from experiment (%)	:	0.1680
Wt percent of precipitated asp. from calculation (%)	:	0.1316

APPENDIX B – Continued

Core data	:	Core 13
L(cm)	:	0.94
D(cm)	:	3.8
Area (cm2)	:	11.3426
Bulk volume(cc)	:	10.6607
Dry weight(g)	:	16.6291
Sat weight(g)	:	20.3900
PV(ml)	:	4.3386
Density of oil @15^{o}C(g/cc)	:	0.8668
Porosity (%)	:	41
Inject. press(bar)	:	100
Confining press(bar)	:	120
Delta press (inlet - outlet) (bar)	:	1
Temp(^{o}C)	:	40
Refractive index before flooding	:	1.482770
Refractive index after flooding	:	1.473715
Delta Refractive Index	:	0.009055
Wt of asp. inside the core before flooding (g)	:	0.0089
Wt of asp. inside the core after flooding (g)	:	0.0011
Wt of asp. In the liquid after flooding (g)	:	0.0078
Total mass of CO_2 injected (g)	:	65
Mol % of CO_2	:	73.4
Wt of core after flooding and drying (g)	:	16.6302
Wt percent of precipitated asp. from experiment (%)	:	0.0254
Wt percent of precipitated asp. from calculation (%)	:	0.0202

APPENDIX B – Continued

Core data	:	Core 14
L(cm)	:	0.91
D(cm)	:	3.8
Area (cm2)	:	11.3426
Bulk volume(cc)	:	10.3205
Dry weight(g)	:	15.1783
Sat weight(g)	:	19.1300
PV(ml)	:	4.5587
Density of oil @15^{o}C(g/cc)	:	0.8668
Porosity (%)	:	44
Inject. press(bar)	:	100
Confining press(bar)	:	120
Delta press (inlet - outlet) (bar)	:	2
Temp(^{o}C)	:	40
Refractive index before flooding	:	1.482770
Refractive index after flooding	:	1.471715
Delta Refractive Index	:	0.011055
Wt of asp. inside the core before flooding (g)	:	0.0093
Wt of asp. inside the core after flooding (g)	:	0.0031
Wt of asp. In the liquid after flooding (g)	:	0.0062
Total mass of CO_2 injected (g)	:	71
Mol % of CO_2	:	73.4
Wt of core after flooding and drying (g)	:	15.1814
Wt percent of precipitated asp. from experiment (%)	:	0.0680
Wt percent of precipitated asp. from calculation (%)	:	0.0541

APPENDIX B – Continued

Core data	:	Core 15
L(cm)	:	0.925
D(cm)	:	3.8
Area (cm2)	:	11.3426
Bulk volume(cc)	:	10.4906
Dry weight(g)	:	15.2493
Sat weight(g)	:	19.2300
PV(ml)	:	4.5922
Density of oil @15^{o}C(g/cc)	:	0.8668
Porosity (%)	:	44
Inject. press(bar)	:	100
Confining press(bar)	:	120
Delta press (inlet - outlet) (bar)	:	4
Temp(^{o}C)	:	40
Refractive index before flooding	:	1.482770
Refractive index after flooding	:	1.461240
Delta Refractive Index	:	0.02153
Wt of asp. inside the core before flooding (g)	:	0.0094
Wt of asp. inside the core after flooding (g)	:	0.0072
Wt of asp. In the liquid after flooding (g)	:	0.0022
Total mass of CO_2 injected (g)	:	97
Mol % of CO_2	:	73.4
Wt of core after flooding and drying (g)	:	15.2565
Wt percent of precipitated asp. from experiment (%)	:	0.1568
Wt percent of precipitated asp. from calculation (%)	:	0.1248

APPENDIX B – Continued

Core data	:	Core 16
L(cm)	:	0.955
D(cm)	:	3.8
Area (cm2)	:	11.3426
Bulk volume(cc)	:	10.8308
Dry weight(g)	:	15.9264
Sat weight(g)	:	20.0400
PV(ml)	:	4.7455
Density of oil @15°C(g/cc)	:	0.8668
Porosity (%)	:	44
Inject. press(bar)	:	110
Confining press(bar)	:	130
Delta press (inlet - outlet) (bar)	:	1
Temp(°C)	:	40
Refractive index before flooding	:	1.482770
Refractive index after flooding	:	1.474725
Delta Refractive Index	:	0.008045
Wt of asp. inside the core before flooding (g)	:	0.0097
Wt of asp. inside the core after flooding (g)	:	0.0012
Wt of asp. In the liquid after flooding (g)	:	0.0085
Total mass of CO_2 injected (g)	:	79
Mol % of CO_2	:	73.5
Wt of core after flooding and drying (g)	:	15.9276
Wt percent of precipitated asp. from experiment (%)	:	0.0253
Wt percent of precipitated asp. from calculation (%)	:	0.0205

APPENDIX B – Continued

Core data	:	Core 17
L(cm)	:	0.965
D(cm)	:	3.8
Area (cm2)	:	11.3426
Bulk volume(cc)	:	10.9442
Dry weight(g)	:	15.7445
Sat weight(g)	:	19.9400
PV(ml)	:	4.8400
Density of oil @15^{o}C(g/cc)	:	0.8668
Porosity (%)	:	44
Inject. press(bar)	:	110
Confining press(bar)	:	130
Delta press (inlet - outlet) (bar)	:	2
Temp(^{o}C)	:	40
Refractive index before flooding	:	1.482770
Refractive index after flooding	:	1.471725
Delta Refractive Index	:	0.011045
Wt of asp. inside the core before flooding (g)	:	0.0099
Wt of asp. inside the core after flooding (g)	:	0.0026
Wt of asp. In the liquid after flooding (g)	:	0.0073
Total mass of CO_2 injected (g)	:	94
Mol % of CO_2	:	73.5
Wt of core after flooding and drying (g)	:	15.7471
Wt percent of precipitated asp. from experiment (%)	:	0.0537
Wt percent of precipitated asp. from calculation (%)	:	0.0435

APPENDIX B – Continued

Core data	:	Core 18
L(cm)	:	1.12
D(cm)	:	3.8
Area (cm2)	:	11.3426
Bulk volume(cc)	:	12.7021
Dry weight(g)	:	18.3274
Sat weight(g)	:	23.2700
PV(ml)	:	5.7019
Density of oil @15^{o}C(g/cc)	:	0.8668
Porosity (%)	:	45
Inject. press(bar)	:	110
Confining press(bar)	:	130
Delta press (inlet - outlet) (bar)	:	4
Temp(^{o}C)	:	40
Refractive index before flooding	:	1.482770
Refractive index after flooding	:	1.463725
Delta Refractive Index	:	0.019045
Wt of asp. inside the core before flooding (g)	:	0.0117
Wt of asp. inside the core after flooding (g)	:	0.0083
Wt of asp. In the liquid after flooding (g)	:	0.0034
Total mass of CO_2 injected (g)	:	87
Mol % of CO_2	:	73.5
Wt of core after flooding and drying (g)	:	18.3357
Wt percent of precipitated asp. from experiment (%)	:	0.1456
Wt percent of precipitated asp. from calculation (%)	:	0.1180

APPENDIX B – Continued

Core data	:	Core 19
L(cm)	:	0.97
D(cm)	:	3.8
Area (cm2)	:	11.3426
Bulk volume(cc)	:	11.0009
Dry weight(g)	:	15.4524
Sat weight(g)	:	19.6800
PV(ml)	:	4.8770
Density of oil @15^{o}C(g/cc)	:	0.8668
Porosity (%)	:	44
Inject. press(bar)	:	90
Confining press(bar)	:	110
Delta press (inlet - outlet) (bar)	:	1
Temp(^{o}C)	:	30
Refractive index before flooding	:	1.482770
Refractive index after flooding	:	1.47272
Delta Refractive Index	:	0.010050
Wt of asp. inside the core before flooding (g)	:	0.0100
Wt of asp. inside the core after flooding (g)	:	0.0015
Wt of asp. In the liquid after flooding (g)	:	0.0085
Total mass of CO_2 injected (g)	:	81
Mol % of CO_2	:	73.9
Wt of core after flooding and drying (g)	:	15.4539
Wt percent of precipitated asp. from experiment (%)	:	0.0308
Wt percent of precipitated asp. from calculation (%)	:	0.0246

APPENDIX B – Continued

Core data	:	Core 20
L(cm)	:	0.88
D(cm)	:	3.8
Area (cm2)	:	11.3426
Bulk volume(cc)	:	9.9802
Dry weight(g)	:	14.6702
Sat weight(g)	:	18.4300
PV(ml)	:	4.3374
Density of oil @15^{o}C(g/cc)	:	0.8668
Porosity (%)	:	43
Inject. press(bar)	:	90
Confining press(bar)	:	110
Delta press (inlet - outlet) (bar)	:	2
Temp(^{o}C)	:	30
Refractive index before flooding	:	1.482770
Refractive index after flooding	:	1.467605
Delta Refractive Index	:	0.0152
Wt of asp. inside the core before flooding (g)	:	0.0089
Wt of asp. inside the core after flooding (g)	:	0.0031
Wt of asp. In the liquid after flooding (g)	:	0.0058
Total mass of CO_2 injected (g)	:	70
Mol % of CO_2	:	73.9
Wt of core after flooding and drying (g)	:	14.6733
Wt percent of precipitated asp. from experiment (%)	:	0.0715
Wt percent of precipitated asp. from calculation (%)	:	0.0572

APPENDIX B – Continued

Core data	:	Core 21
L(cm)	:	0.87
D(cm)	:	3.8
Area (cm2)	:	11.34262
Bulk volume(cc)	:	9.86682312
Dry weight(g)	:	14.2747
Sat weight(g)	:	18.08
PV(ml)	:	4.389852799
Density of oil @15°C(g/cc)	:	0.86684
Porosity (%)	:	44.49104585
Inject. press(bar)	:	90
Confining press(bar)	:	110
Delta press (inlet - outlet) (bar)	:	4
Temp(°C)	:	30
Refractive index before flooding	:	1.482770
Refractive index after flooding	:	1.46367
Delta Refractive Index	:	0.019100
Wt of asp. inside the core before flooding (g)	:	0.0089956
Wt of asp. inside the core after flooding (g)	:	0.0067
Wt of asp. In the liquid after flooding (g)	:	0.0023
Total mass of CO_2 injected (g)	:	90
Mol % of CO_2	:	73.9
Wt of core after flooding and drying (g)	:	14.2814
Wt percent of precipitated asp. from experiment (%)	:	0.152624708
Wt percent of precipitated asp. from calculation (%)	:	0.122245676

APPENDIX B – Continued

Core data	:	Core 22
L(cm)	:	0.88
D(cm)	:	3.8
Area (cm2)	:	11.3426
Bulk volume(cc)	:	9.9802
Dry weight(g)	:	14.3966
Sat weight(g)	:	18.3000
PV(ml)	:	4.5030
Density of oil @15^{o}C(g/cc)	:	0.8668
Porosity (%)	:	45
Inject. press(bar)	:	100
Confining press(bar)	:	120
Delta press (inlet - outlet) (bar)	:	1
Temp(^{o}C)	:	30
Refractive index before flooding	:	1.482770
Refractive index after flooding	:	1.473725
Delta Refractive Index	:	0.009045
Wt of asp. inside the core before flooding (g)	:	0.0092
Wt of asp. inside the core after flooding (g)	:	0.0009
Wt of asp. In the liquid after flooding (g)	:	0.0083
Total mass of CO_2 injected (g)	:	80
Mol % of CO_2	:	74.0
Wt of core after flooding and drying (g)	:	14.3975
Wt percent of precipitated asp. from experiment (%)	:	0.0200
Wt percent of precipitated asp. from calculation (%)	:	0.0162

APPENDIX B – Continued

Core data	:	Core 23
L(cm)	:	1.19
D(cm)	:	3.8
Area (cm2)	:	11.3426
Bulk volume(cc)	:	13.4960
Dry weight(g)	:	18.9578
Sat weight(g)	:	24.2000
PV(ml)	:	6.0475
Density of oil @15^{o}C(g/cc)	:	0.8668
Porosity (%)	:	45
Inject. press(bar)	:	100
Confining press(bar)	:	120
Delta press (inlet - outlet) (bar)	:	2
Temp(^{o}C)	:	30
Refractive index before flooding	:	1.482770
Refractive index after flooding	:	1.467695
Delta Refractive Index	:	0.015075
Wt of asp. inside the core before flooding (g)	:	0.0124
Wt of asp. inside the core after flooding (g)	:	0.0033
Wt of asp. In the liquid after flooding (g)	:	0.0091
Total mass of CO_2 injected (g)	:	76
Mol % of CO_2	:	74.0
Wt of core after flooding and drying (g)	:	18.9611
Wt percent of precipitated asp. from experiment (%)	:	0.0546
Wt percent of precipitated asp. from calculation (%)	:	0.0441

APPENDIX B – Continued

Core data	:	Core 24
L(cm)	:	0.93
D(cm)	:	3.8
Area (cm2)	:	11.3426
Bulk volume(cc)	:	10.5473
Dry weight(g)	:	15.1945
Sat weight(g)	:	19.2200
PV(ml)	:	4.6439
Density of oil @15^{o}C(g/cc)	:	0.8668
Porosity (%)	:	44
Inject. press(bar)	:	100
Confining press(bar)	:	120
Delta press (inlet - outlet) (bar)	:	4
Temp(^{o}C)	:	30
Refractive index before flooding	:	1.482770
Refractive index after flooding	:	1.463695
Delta Refractive Index	:	0.019075
Wt of asp. inside the core before flooding (g)	:	0.0095
Wt of asp. inside the core after flooding (g)	:	0.0066
Wt of asp. In the liquid after flooding (g)	:	0.0029
Total mass of CO_2 injected (g)	:	67
Mol % of CO_2	:	74.0
Wt of core after flooding and drying (g)	:	15.2011
Wt percent of precipitated asp. from experiment (%)	:	0.1421
Wt percent of precipitated asp. from calculation (%)	:	0.1150

APPENDIX B – Continued

Core data	:	Core 25
L(cm)	:	0.88
D(cm)	:	3.8
Area (cm2)	:	11.3426
Bulk volume(cc)	:	9.9802
Dry weight(g)	:	14.5650
Sat weight(g)	:	18.2600
PV(ml)	:	4.2626
Density of oil @15^{o}C(g/cc)	:	0.8668
Porosity (%)	:	43
Inject. press(bar)	:	110
Confining press(bar)	:	130
Delta press (inlet - outlet) (bar)	:	1
Temp(^{o}C)	:	30
Refractive index before flooding	:	1.482770
Refractive index after flooding	:	1.47372
Delta Refractive Index	:	0.009050
Wt of asp. inside the core before flooding (g)	:	0.0087
Wt of asp. inside the core after flooding (g)	:	0.0008
Wt of asp. In the liquid after flooding (g)	:	0.0079
Total mass of CO_2 injected (g)	:	67
Mol % of CO_2	:	74.1
Wt of core after flooding and drying (g)	:	14.5658
Wt percent of precipitated asp. from experiment (%)	:	0.0188
Wt percent of precipitated asp. from calculation (%)	:	0.0153

APPENDIX B – Continued

Core data	:	Core 26
L(cm)	:	0.86
D(cm)	:	3.8
Area (cm2)	:	11.3426
Bulk volume(cc)	:	9.7534
Dry weight(g)	:	14.2744
Sat weight(g)	:	17.9300
PV(ml)	:	4.2172
Density of oil @15^{o}C(g/cc)	:	0.8668
Porosity (%)	:	43
Inject. press(bar)	:	110
Confining press(bar)	:	130
Delta press (inlet - outlet) (bar)	:	2
Temp(^{o}C)	:	30
Refractive index before flooding	:	1.482770
Refractive index after flooding	:	1.468715
Delta Refractive Index	:	0.014055
Wt of asp. inside the core before flooding (g)	:	0.0086
Wt of asp. inside the core after flooding (g)	:	0.0020
Wt of asp. In the liquid after flooding (g)	:	0.0066
Total mass of CO_2 injected (g)	:	75
Mol % of CO_2	:	74.1
Wt of core after flooding and drying (g)	:	14.2764
Wt percent of precipitated asp. from experiment (%)	:	0.0474
Wt percent of precipitated asp. from calculation (%)	:	0.0387

APPENDIX B – Continued

Core data	:	Core 27
L(cm)	:	0.89
D(cm)	:	3.8
Area (cm2)	:	11.3426
Bulk volume(cc)	:	10.0936
Dry weight(g)	:	14.6499
Sat weight(g)	:	18.5100
PV(ml)	:	4.4531
Density of oil @15^{o}C(g/cc)	:	0.8668
Porosity (%)	:	44
Inject. press(bar)	:	110
Confining press(bar)	:	130
Delta press (inlet - outlet) (bar)	:	4
Temp(^{o}C)	:	30
Refractive index before flooding	:	1.482770
Refractive index after flooding	:	1.465505
Delta Refractive Index	:	0.017265
Wt of asp. inside the core before flooding (g)	:	0.0091
Wt of asp. inside the core after flooding (g)	:	0.0062
Wt of asp. In the liquid after flooding (g)	:	0.0029
Total mass of CO_2 injected (g)	:	95
Mol % of CO_2	:	74.1
Wt of core after flooding and drying (g)	:	14.6561
Wt percent of precipitated asp. from experiment (%)	:	0.1392
Wt percent of precipitated asp. from calculation (%)	:	0.1137